9-1-2020

Phylogenomic Analysis Of Evolutionary Relationships In Ranitomeya Poison Frogs (Amphibia: Dendrobatidae) Using Ultraconserved Elements

Morgan Renee Muell
Southern Illinois University Carbondale, morganrmuell@gmail.com

PHYLOGENOMIC ANALYSIS OF EVOLUTIONARY RELATIONSHIPS IN *RANITOMEYA* POISON FROGS (AMPHIBIA: DENDROBATIDAE) USING ULTRACONSERVED ELEMENTS

by

Morgan R. Muell

B.S., Iowa State University, 2018

A Thesis
Submitted in Partial Fulfillment of the Requirements for the
Master of Science Degree

School of Biological Sciences
in the Graduate School
Southern Illinois University Carbondale
August 2020

THESIS APPROVAL

PHYLOGENOMIC ANALYSIS OF EVOLUTIONARY RELATIONSHIPS IN *RANITOMEYA* POISON FROGS (AMPHIBIA: DENDROBATIDAE) USING ULTRACONSERVED ELEMENTS

by

Morgan R. Muell

A Thesis Submitted in Partial

Fulfillment of the Requirements

for the Degree of

Master of Science

in the field of Zoology

Approved by:

Dr. Jason L. Brown, Chair

Dr. Frank E. Anderson

Dr. Francisco Agustín Jiménez-Ruiz

Graduate School
Southern Illinois University Carbondale
June 11, 2020

AN ABSTRACT OF THE THESIS OF

Morgan R. Muell, for the Master of Science degree in Zoology, presented on June 11, 2020, at Southern Illinois University Carbondale.

TITLE: PHYLOGENOMIC ANALYSIS OF EVOLUTIONARY RELATIONSHIPS IN *RANITOMEYA* POISON FROGS (AMPHIBIA: DENDROBATIDAE) USING ULTRACONSERVED ELEMENTS

MAJOR PROFESSOR: Dr. Jason L. Brown

Knowledge of phylogenetic relationships among organisms is essential for anchoring evolutionary studies. Phylogenomic studies use large amounts of genetic data in analyses, which is particularly important for highly phenotypically variable taxa that are difficult to distinguish from one another without the use of genetic data, due to the abundance of homoplasy in morphological characters typically used in morphological classification. Use of genome-scale molecular data has thus become the gold standard for identifying these phylogenetic relationships, specifically in comparison to past studies based on fewer genes. Greater quantities of genetic data, in addition to finer taxon sampling, may lead to different conclusions about phylogenetic relationships among organisms compared to previous studies, necessitating new analyses on organisms when new discoveries of populations and new sources of genetic data arise. *Ranitomeya* poison frogs (Amphibia: Dendrobatidae) are an Amazonian lineage of dendrobatid frogs consisting of 16 species possessing remarkable diversity in color pattern, range size, and parental care behavior. I present the first phylogeny based on genomic data for all species in *Ranitomeya*, using maximum likelihood and multi-species coalescent methods. I used ultraconserved elements (UCEs), a genome-scale nuclear marker, as my source of molecular data to construct the tree. I also present divergence time estimations using the MCMCTree program. My results indicate several differences from previous analyses in terms of interspecific relationships. Notably, I find *R. toraro* and *R. defleri* constitute different species groups, and

recover *R. uakarii* as paraphyletic. I also designate former populations of *R. fantastica* from Isla Pongo, Peru and Tarapoto as *R. summersi*, and transfer the French Guianan *R. amazonica* populations to *R. variabilis*. My study clarifies both interspecific and intraspecific relationships within *Ranitomeya*, and provides key insights into phylogeny that pave the way for future studies testing hypotheses on color pattern evolution and historical biogeography.

ACKNOWLEDGMENTS

I am indebted to Germán Chávez and Ivan Prates for providing many samples for my dataset, without which this work would not have been possible, as well as Dr. Evan Twomey for providing samples and important insights about these results. I thank Miguel T. Rodrigues at Universidade de São Paulo, Janalee Caldwell at Sam Noble Oklahoma Museum of Natural History, César Aguilar at Museo de Historia Natural in Lima, Peru, and Kyle Summers at East Carolina University for providing additional specimens for my analysis. I also thank Andrew J. Mason for fielding my questions on divergence time estimation using PAML.

I owe huge thanks to the Students United in Exploring, Preserving, and Researching Biodiversity (SUPERB) fellowship for their community, and for funding my research from 2019-2020 (NSF Grant DUE-1564969). I also thank the Zoology division of the School of Biological Sciences for funding my summer research in 2019 on the Zoology Summer Scholarship. Permits were issued by: Brazil's Instituto Chico Mendes de Conservação da Biodiversidade (SISBIO 30309, 36753, 7147) the Servicio Nacional Forestal y de Fauna Silvestre in Peru (R.D.G. 120- 2012-AG-DGFFS-DGEFFS, R.D.G. 029-2016-SERFOR-DGGSPFFS, R.D.G. 405-2016-SERFOR-DGGSPFFS, R.D.G. 116-2017-SERFORDGGSPFFS, N° 002765-AG-INRENA, N° 061-2003-INRENA-IFFS-DCB, N° 050-2006-INRENA-IFFS-DCB, N° 067-2007-INRENA-IFFS-DCB, N° 083-2017-SERFOR/DGGSPFFS, N°004-2013-SERNANP-JRCA, and N°016-2010-SERNANP-DGANP), Contrato de Acceso Marco a Recursos Genéticos in Peru (359-2013-MINAGRI-DGFFS-DGEFFS, Ministerio de Agricultura of Peru (Permit Number Code 25397, N° 2904-2012-AGDGFFS-DGEFFS) and the administration of Manu National Park (06-2013-SERNANP-PNM-JEF)

I am so grateful for my fellow students in the graduate program at SIU for their

friendship and sense of community. I am particularly grateful for Andrew O. Rubio for his companionship and all our conversations about these incredible poisonous frogs. Moreover, I owe thanks beyond measure to my lab big brother Wilson X. Guillory, whose patience, bioinformatic wizardry, and steadfast friendship pulled me through the toughest moments of this journey. Lastly, I am thankful for the Brown Lab, which cultivated an atmosphere that continually challenged my perceptions, encouraged boundless curiosity, creativity and confidence, and instilled in me the uncompromising spirit to pursue the kind of scientific career I am proud of. I couldn't have asked for a better lab to call home!

TABLE OF CONTENTS

LIST OF TABLES

TABLE PAGE

LIST OF FIGURES

CHAPTER 1

INTRODUCTION

Understanding the maintenance and generation of biodiversity remains a central goal in evolutionary biology. Phenotypic diversity represents a particular challenge to understand, owing to the diversity of mechanisms contributing to phenotypic diversity. Polytypic organisms, species with great intraspecific phenotypic variation, offer golden opportunities for understanding speciation processes, patterns of hybridization, and phenotypic evolution. For example, insights into relationships among *Heliconius* butterflies using whole-genome data have yielded great insights into generation and maintenance of mimicry rings as well as speciation (Jiggins 2008, Enciso-Romero et al. 2017). In vertebrates, examining genetic structure among highly variable populations of strawberry poison frogs (*Oophaga pumilio*) has shown the importance of phenotypic variation in divergence events, suggesting the importance of sexual selection in phenotypic diversification among some species (Wang and Summers 2010).

Aposematic vertebrates offer a double dose of mystery for understanding phenotype diversification because of the combatting forces affecting phenotype generation. Predation risk would suggest that a uniform warning signal is ideal to project across all organisms in a species, to accelerate predator learning to avoid eating that distasteful organism. However, many aposematic organisms still exhibit remarkable variation in color and pattern. For example, as mentioned above, strawberry poison frogs (*Oophaga pumilio*) have diversified into many morphs across islands in the Bocas del Toro region of Costa Rica (Daly and Myers 1967), and *Dendrobates auratus* poison frogs have diversified to a great variety of phenotypes from Nicaragua through Panama and northern Colombia (Savage 2002). Several alternative hypotheses have been suggested and tested to explain this diversity in phenotype (Lawrence et

al. 2019). These include sexual selection, namely female mate choice (Crothers and Cummings 2013), and differences in optimal warning signals for different predators (Mallet and Joron 1999). Much work remains to be done to identify drivers of patterns in phenotypic diversity among aposematic organisms, and particularly in poison frogs. Despite notable scientific attention, there remain many unanswered questions about their evolutionary relationships and how their many species have diversified. The potential for considerable intraspecific variation has challenged systematists (e.g., see Wollenberg et al. 2006), especially in absence of genetic data. Systematic revisions, and studies of color-pattern and mating system evolution require detailed and robust estimates of evolutionary relationships among species and populations.

Ranitomeya is a genus of poison frogs that includes 16 species distributed throughout the Amazon rainforest, and is characterized by diminutive size, pale reticulated limbs, and first fingers being shorter than second fingers (Brown et al. 2011b). Some species possess astounding intraspecific diversity in color pattern, sometimes including up to four recognized morphs, and even a propensity to selectively mate with similar morphs (Twomey et al. 2016). However, many other species in the genus are monotypic. Phenotypic diversity is not tied to size of species geographic range; there are monotypic species with insular (e.g., *R. yavaricola*) and wide ranges (e.g., *R. toraro*) ranges, and polytypic species with insular (e.g., *R. imitator*, *R. fantastica*) and wide (e.g., *R. variabilis*, *R. uakarii*) ranges. Most species occupy forested areas near the Andes in Peru, Ecuador, and Colombia, though some species have dispersed outward into Brazil and further penetrated the Amazon far east into French Guiana to occupy a continental distribution (Brown et al. 2011b). Multiple types of mating systems and parental care types have also evolved within the group. The *vanzolinii* species group includes several species with monogamous mating pairs and biparental care, such as *R. imitator* and *R. vanzolinii*, whereas

members of the *reticulata* species group as well as *R. sirensis* in the *vanzolinii* group are promiscuous species with male-only parental care (Brown et al. 2011b). The great diversity in phenotype, behavior, and biogeographic history that *Ranitomeya* possesses make the genus an endless fountain of exciting evolutionary questions.

Historically, delimiting species boundaries within *Ranitomeya* has proven difficult for several reasons. First, contrary to their huge diversity in color and pattern, they display remarkably little osteological or any other morphological diversity, limiting the utility of morphological data for use in phylogenetic analysis. Second, complicated histories of color pattern evolution have led to an abundance of Müllerian mimicry among species, which in addition to high levels of sympatry have made similar-looking species difficult to classify. One famous example is *R. imitator*, which mimics the color and pattern of both *R. fantastica* and *R. variabilis* in several areas of its range, though species other than *R. imitator* also potentially feature in Müllerian mimic pairs (e.g., *R. reticulata* and *R. amazonica*) (Brown et al. 2011b). Thus, genetic data is absolutely essential to understanding the underlying evolutionary relationships of the genus, and the evolving nature of genetic data availability and phylogenetic methods have determined the history of *Ranitomeya* taxonomy and systematics.

The first two described species in *Ranitomeya*, *R. reticulata* and *R. fantastica*, were described by Boulenger (1883), long before the advent of genetic resources. Despite this early description, initial systematic studies on *Dendrobates*, which included *Ranitomeya* sensu Grant et al. (2006), were not completed until around 100 years later, based on morphological characters (Silverstone 1975). Wary on account of their astounding color and pattern diversity, early researchers conservatively grouped *Ranitomeya* specimens into *Dendrobates* in an attempt to avoid describing too many species based simply on color and pattern. More studies followed that

incorporated alkaloid profiles, vocalizations, and behavioral data into their classifications (Myers and Daly 1980, Myers 1982). Phylogenetic studies that included molecular data on samples of species currently recognized in the *Ranitomeya* genus did not begin until the late 1990s.

Kyle Summers and colleagues began initial phylogenetic studies into relationships among *Dendrobates* species, which included *Ranitomeya* at the time, using mitochondrial sequence data and parsimony techniques (Summers et al. 1997, Summers et al. 1999, Clough and Summers 2000). These pioneering studies clarified relationships among represented *Ranitomeya* taxa, which at the time included *R. vanzolinii*, *R. fantastica*, and *R. ventrimaculata*. Vences et al. (2000) also used parsimony and mitochondrial data (from the 16S region) in a parsimony analysis on relationships among the Dendrobatidae family, and found *R. imitator* (then *Dendrobates*) was sister to *Minyobates fulguritus*, now a member of *Andinobates*, an early insight into the most recently supported intergeneric relationships sensu Brown et al. (2011b). Symula and colleagues went on to examine relationships in *Dendrobates* with greater representation of geographic and morphological diversity, adding maximum likelihood and neighbor-joining methods (Symula et al. 2001, Symula et al. 2003), and began discussing biogeographic history of the group (Symula et al. 2003). Santos et al. (2003) also evaluated branch support for the clades in *Ranitomeya* more comprehensively in an analysis on *Dendrobates*, with additional mitochondrial data and Bayesian methods, and found similar results to other initial phylogenetic studies. Additional earlier studies also employed likelihood and Bayesian-based methods (Darst and Cannatella 2004). These earlier studies provided well vetted hypotheses for later analyses, but their insights are restricted by limited taxon sampling, as they took place prior to the description of many currently recognized species.

In 2006, many more studies began interrogating the evolutionary relationships among

Ranitomeya. In their pivotal publication on dendrobatid systematics, Grant et al. (2006) split apart the *Dendrobates* genus and erected the *Ranitomeya* genus, though their findings on interspecific relationships in *Ranitomeya* are not consistent with other analyses focused more closely on *Ranitomeya* and closely related genera (e.g., Twomey and Brown 2008, Perez-Peña et al. 2010, Brown et al. 2011b). Studies that followed included much more comprehensive taxon sampling to elucidate relationships, using mitochondrial data and likelihood-based methods (Noonan and Wray 2006, Roberts et al. 2006), or a combination of mitochondrial and nuclear data with likelihood-based methods (Twomey and Brown 2008). Many species descriptions also followed close behind in accordance with evidence from molecular data, including the descriptions of *R. uakarii* (Brown et al. 2006), *R. benedicta and R. summersi* (Brown et al. 2008), *R. defleri* (Twomey and Brown 2009), *R. yavaricola* and *R. cyanovittata* (Perez-Peña et al. 2010). These species descriptions helped lay the framework for additionally thorough taxon sampling in subsequent phylogenetic analyses in *Ranitomeya*. Many of these later studies corroborated alpha-taxonomic relationships posited by earlier studies, and provided hypotheses for the standing of new species and newly discovered populations of previously described species.

Santos et al. (2009) advanced phylogenetic analyses on dendrobatids much further by calculating divergence time estimates for all of Dendrobatidae, including *Ranitomeya*. Not long after, Brown et al. (2011b) comprehensively revised *Ranitomeya* relationships in their monograph using Bayesian analyses on nuclear and mitochondrial data. They made several major systematic changes, including splitting off the genus *Andinobates*, describing *R. toraro*, and synonymizing *R. lamasi* and *R. biolat* sensu Morales (1992) into *R. sirensis*. Since this work, the frequency of phylogenetic studies on *Ranitomeya* has slowed. Grant et al. (2017) revisited

relationships among all of Dendrobatidae using a parsimony analysis, finding slightly different clade-level relationships than those in Brown et al. (2011b), and Guillory et al. (2019) published the first study incorporating genomic-scale molecular data into an analysis of Dendrobatidae that included some *Ranitomeya* species.

Major questions still exist regarding interspecific relationships within some groups in *Ranitomeya* that conflicted among previous studies that used different phylogenetic methods and different sources of genetic data. For example, *R. toraro* was placed sister to *R. defleri* in a species group sister to the *reticulata* clade when first described by Brown et al. (2011b). However, Grant et al. (2017) found that this species group was sister to the *variabilis* group, not the *reticulata* group. Thus, the placement of *R. toraro* and *R. defleri* in the phylogeny remain unclear. Further, the *reticulata* species group requires revisiting, particularly in regard to the status of *R. uakarii*. Preliminary analysis on morphology suggests a divide between the northern and southern populations of *R. uakarii* (Brown et al. 2011b, Brown et al. unpub. data), necessitating reevaluation of the species. Lastly, relationships in the *vanzolinii* group are in flux. Particularly, placement of *R. yavaricola* and *R. cyanovittata* in relation to other species in the *vanzolinii* group have varied in studies since their description by Perez-Peña et al. (2010) (Brown et al. 2011b, Grant et al. 2017). Fine-scale taxon sampling is necessary to answer each of these outstanding questions, and could potentially contribute other insights into inter- and intra-specific relatedness beyond a priori systematic issues.

There have been no studies on *Ranitomeya* phylogeny that both use genome-scale data and have comprehensive taxon sampling across all species in the genus. Almost all previous studies on *Ranitomeya* phylogeny have used mitochondrial data (Summers et al. 1997, Summers et al. 1999, Clough and Summers 2000, Vences et al. 2000, Symula et al. 2001, Santos et al.

2003, Symula et al. 2003, Darst and Cannatella 2004, Noonan and Wray 2006, Roberts et al. 2006) or a combination of mitochondrial data with nuclear loci (Grant et al. 2006, Twomey and Brown 2008, Santos et al. 2009, Perez-Peña et al. 2010, Brown et al. 2011b, Pyron and Wiens 2011, Grant et al. 2017) or morphological characters (Brown et al. 2008). A genomic analysis of *Ranitomeya* has yet to be done with all the species in the genus that also includes comprehensive representative sampling spanning the large geographic ranges and great color pattern variation some species exhibit. Guillory et al. (2019) used ultraconserved elements to generate a phylogeny for all of Dendrobatidae, which included *Ranitomeya* samples, but not all species were represented. Their success using ultraconserved elements on *Ranitomeya* samples shows promise for another success using genome-scale data for phylogenetic analysis for all of *Ranitomeya*. A genomic analysis is of great utility to help solve remaining systematic issues with the group, and anchor applied studies using phylogeny.

In this thesis, I generated a phylogeny on the *Ranitomeya* genus using genomic-scale molecular data, a diversity of phylogenetic methods, and comprehensive taxon sampling of genetic, morphological, and geographic diversity across the genus. I used ultraconserved elements (UCEs) as my genomic data source because of their high utility at both shallow and deep evolutionary timescales (Faircloth et al. 2012). UCEs consist of a highly conserved sequence region with flanking sequences of increasing variability as distance from the conserved region increases, and have been used successfully in previous studies of dendrobatid phylogeny (Guillory et al. 2019, Guillory et al. 2020). I used UCEs in maximum likelihood, multispecies coalescent, and divergence time estimation analyses to investigate phylogenetic relationships in *Ranitomeya*.

CHAPTER 2

MATERIALS AND METHODS

Data Collection

I used previously collected DNA samples from 65 *Ranitomeya* individuals. These individuals broadly represent the known genetic, geographic, and phenotypic diversity exhibited across the genus (Table S1). One sample of *Andinobates minutus* (sister genus to *Ranitomeya*; Brown et al. 2011b) and one sample of *Excidobates captivus* (sister genus to *Andinobates* and *Ranitomeya*; Guillory et al. 2019) served as outgroup taxa, for a total of 67 samples in the tree. Photo vouchers were collected for all sequenced individuals upon collection of the DNA sample. DNA was extracted from poison frog toe tissue using the Qiagen DNeasy Blood and Tissue Kit (Valencia, California), and sent off to RAPiD Genomics (Gainesville, Florida), where they carried out Illumina sequencing of ultraconserved elements (UCEs). I used the Tetrapods-UCE-5Kv1 probe set to enrich the samples and target 5060 UCE loci using 5472 probes.

Bioinformatics

After obtaining raw reads of sequences from RAPiD Genomics, I trimmed reads using Illumiprocessor version 2.0.6 (Faircloth 2013) through the software PHYLUCE v1.5.0 using default parameters (Faircloth 2016). Illumiprocessor is a Python-based program used to implement the software Trimmomatic version 0.36 (Bolger et al. 2014). To assemble the trimmed reads, I used Trinity version 1.6 (Grabherr et al. 2011), using default parameters. I mapped these assembled contigs to UCE loci, also using PHYLUCE, and individually aligned each locus using MUSCLE v3.8.31 using default parameters (Edgar 2004). I initially filtered captured loci for 70% matrix completeness, which retained only loci that were present in at least 70% of my samples. I then filtered the remaining loci further for the top 75% most informative

loci based on parsimony-informative sites, which removed the lower 25% of the distribution with the lowest numbers of parsimony-informative sites. Both these steps helped to prevent inaccurate results in my coalescent-based analysis due to the influence of less-informative loci (Hosner et al. 2016). To filter for informativeness, I used the PHYLOCH package v1.5-5 (Heibl 2008) in R version 3.2.3 (R Core Team 2015), and used the resulting dataset for all my analyses.

I performed trials using different percentage thresholds for matrix completeness and data informativeness to evaluate whether my chosen thresholds were appropriate. As previously mentioned, some literature suggests that using loci with low-informative sites result in incorrect topologies and lower support values, particularly in coalescent-based analyses (Hosner et al. 2016), which is why I chose to retain the top 75% most informative loci rather than constructing a 95% confidence interval of the dataset based on a normal distribution and filtering out the outliers on the top and bottom of the distribution. I manipulated different filtering thresholds of matrix completeness and locus informativeness to see how different thresholds affected the results. For completeness trials, I kept informativeness constant at the top 75% most informative loci after filtering for differential matrix completeness levels, and altered matrix completeness filtering levels to 50%, 70%, 80%, and 90%. For informativeness trials, I kept completeness filtering constant at 70% prior to altering levels of informativeness filtering. I altered informativeness filtering to the top 50%, 75%, 80%, and 90% most informative loci, as well as loci within a 95% confidence interval of the dataset after filtering for matrix completeness, where I filtered out any outlier loci with very low or very high numbers of parsimony-informative sites. For each trial, I ran an IQ-TREE analysis and an ASTRAL-III analysis and compared the results.

Phylogenetic Analyses

I used several phylogenetic programs to analyze my data. All of my analyses utilized unpartitioned, concatenated matrices. Because UCEs are not protein coding, there is no evidence to support any particular partitioning scheme for them (Streicher and Wiens 2017), and an analysis partitioning by locus was not feasible for all my loci given analysis time constraints. I used IQ-TREE v1.5.5 (Nguyen et al. 2015) as a maximum likelihood method, with a 10,000 bootstrap replicates, GTR substitution model, empirical base frequencies, and the free rate model of rate heterogeneity with 4 categories. I used ModelFinder to determine these were the best-fitting parameters for the IQ-TREE analysis (Kalyaanamoorthy et al. 2017), using AICc as an optimality criterion.

I tested my resulting topology against alternative hypotheses based on previous analyses using the approximately unbiased (AU) topology test (Shimodaira 2002) as implemented in IQ-TREE. I chose to use the AU test as my topology test because it has major advantages over two of its competing alternatives, the Kishino-Hasegawa (KH) test (Kishino and Hasegawa 1989) and the Shimodaira-Hasegawa (SH) test (Shimodaira 2002). The AU test improves on the KH test because it is able to compare the maximum likelihood topology to other possible tree topologies, whereas the KH test cannot due to its assumption that both the trees it is testing are two of a random subset of possible trees with no reference to the genetic dataset at hand. Like the SH test, the AU test compares an alternative hypothesis that some tree topologies in the pool of all possible tree topologies are not equally good explanations of the data against the null hypothesis that all trees in the pool of possible trees are equally good explanations of the data (Goldman et al. 2000). The AU test tends to be less conservative than the SH test in that the AU test does not retain as many possible trees as the SH test does when the pool of trees to compare

increases (Strimmer and Rambaut 2002), eliminating potential biases in tree selection (Shimodaira 2002). However, use of the AU test in the implementation of this study is still limited because the AU test assumes it is testing against a candidate set of trees for comparison, and I have only provided a small subset of possible topologies, violating this assumption of the AU test. The Swofford-Olsen-Waddell-Hillis (SOWH) test implemented with the SOWHAT PERL package (Church et al. 2015) is a possible remedy to this obstacle. The SOWH is a parametric test (unlike the AU test) which tests the alternative hypothesis that a different topology is the true topology against the null hypothesis that the given maximum likelihood topology is the true topology, by simulating replicate datasets based on the parameters provided and subjecting them to the same phylogenetic methods as the original dataset, thus creating replicates for test statistics (Goldman et al. 2000). While very useful and theoretically sound, I was unable to implement the SOWH test due to computational constraints resulting from the size of my genomic dataset. Therefore, I instead chose to move forward with the AU topology test with knowledge of its limitations for interpretation.

I used ASTRAL-III v5.6.1 (Zhang et al. 2018) as a coalescent-based analysis in addition to my IQ-TREE analysis in order to account for incomplete lineage sorting. Each of the 16 currently recognized species in *Ranitomeya*, plus 1 unit to represent southern populations of *R. uakarii*, were designated as coalescent units in the analysis. Prior to the analysis, I used IQ-TREE to generate gene trees for each UCE locus in my filtered dataset to be inputted into the ASTRAL analysis. For each gene tree, I used a GTR model of nucleotide substitution and 1,000 ultrafast bootstrap replicates. I also used IQ-TREE's -czb option, 'collapse zero branch lengths,' to reduce branches with values near zero to polytomies, thereby alleviating the risk of gene tree bias in later analyses (Persons et al. 2016).

Divergence Time Estimation

To calculate divergence time estimates for my dataset, I used MCMCTree in PAML v4.8 (Yang 2007). Divergence time estimations for large genomic-scale datasets can be computationally challenging (see Guillory et al. 2020), and the algorithm MCMCTree uses allowed me to use all the loci captured in my dataset in a computationally feasible amount of time. I used the topology from my maximum likelihood analysis in IQ-TREE as a reference topology, and used an independent rates clock model for rate priors. There is no fossil record for dendrobatid frogs, making calibrating a divergence time estimation analysis challenging. Santos et al. (2009) dated a time-calibrated phylogeny of Dendrobatidae using paleogeographic and fossil calibrations for a dated tree for all of Amphibia, and calculated divergence time estimates for each node in Dendrobatidae under three different paleogeographic scenarios. I averaged three means and three standard deviations of divergence time estimates done across each of these three paleogeographic scenarios for the node corresponding to the divergence of *Ranitomeya* and *Andinobates* from their common ancestor. The mean of the three scenarios was 12.651 million years ago, and the mean standard deviation of 2.576. I used these values to generate a uniform distribution at the calibration node at the divergence between *Ranitomeya* and *Andinobates* between 7.601 and 17.701 million years, corresponding to a 95% confidence interval around the mean. I used the uniform distribution as opposed to a normal distribution because I wanted a diffuse prior with soft bounds on both sides to avoid constraining the analysis too strictly in light of the lack of background information on *Ranitomeya* divergence times. MCMCTree puts hard boundaries on minimum age for normal calibration nodes to treat them as fossils. Using a uniform distribution solves this issue.

I first ran the analysis without sequence data to assess whether my model parameters

produced reasonable priors based on my calibration point. Then, I used BASEML to calculate approximate branch length values prior to running the analysis, using an HKY nucleotide substitution model. I used the HKY model instead of the GTR model previously selected for by ModelFinder in IQ-TREE because BASEML was computationally incapable of performing an analysis using the more complicated GTR model, and the HKY model is the next-closest model to GTR in terms of modeling nucleotide substitution. I ran the MCMCTree analysis for two million burn-in generations and subsequently sampled every 1,000 generations until I had obtained 20,000 samples for a total of 22,000,000 iterations. To assess convergence of the analysis, I ensured ESS values for each node were over 200 for every node I sampled using Tracer v1.7.1 (Rambaut et al. 2018), and I ran the analysis twice on two different random starting seeds.

CHAPTER 3

RESULTS

UCE Sequence Capture

I captured 2,664 loci in my initial dataset. After filtering for 70% matrix completeness, my dataset consisted 1,568 loci. After I filtered these 1,568 loci further for the top 75% most informative loci based on parsimony-informative sites, I retained 1,176 loci consisting of 72,828 parsimony-informative sites for the final dataset.

Completeness and Informativeness Threshold Trials

My completeness and informativeness trials yielded different resulting topologies and support values based on the value manipulated. As expected, a higher threshold for matrix completeness resulted in fewer loci being retained, and increasing the percentage of "top %" loci retained for informativeness trials (e.g., 90% instead of 80%) resulted in retaining more loci (Table 1). Number of parsimony-informative sites naturally increased when more loci were retained (Table 1). For the normal distribution informativeness filtering scheme, the mean number of parsimony-informative sites (PIS) per locus was 51 sites, with a standard deviation of 36 sites, and upper and lower confidence interval bounds between -19 and 120 sites. Because of this negative lower bound, I only retained loci containing between 1 and 120 parsimony-informative sites, resulting in filtering out 75 outlier loci containing more than 120 PIS and no loci on the lower end of the distribution, since no loci qualified as outliers on the lower end of the distribution. The filtering scheme with the best tree likelihood based off my IQ-TREE analysis in the matrix completeness trials was the 70% threshold. Converse to my expectations, the filtering scheme with the best likelihood in the informativeness trials was filtering for the top 50% most informative loci, a dataset with stricter limitations on retaining loci than the top 75%

percent threshold I referenced.

Though all the filtering schemes had noticeably different summary statistics (Table 1), differences in tree topology and support values were minimal among most of the datasets for both maximum likelihood and coalescent analyses. In IQ-TREE analyses, all filtering schemes resulted in the same tree topology and negligible differences in bootstrap support values, except for the 90% matrix completeness topology. This filtering scheme resulted in a radically different topology than the other datasets, including the switch in position between *R. defleri* and *R. toraro*, and placing *R. uakarii* sister to *R. reticulata*. None of the major differences in taxon placement in this tree are supported by previous literature, and this tree also had both one of the worst tree likelihoods and lowest overall bootstrap support values of any of the filtering schemes. For these reasons, I chose to discount these anomalous placements as the result of using a much smaller dataset in comparison to the others. In coalescent analyses, all filtering schemes resulted in the same tree topology. In completeness trials, the 80% and 90% thresholds had overall slightly lower support values than the 70% threshold, and the 50% threshold had slightly higher support values at all nodes except for the common ancestor of *R. reticulata* and the *fantastica* group, where it had a much lower support value of 0.63. In the informativeness trials, the 50% and normal distribution coalescent trees have slightly lower support values overall, and the 75%, 80% and 90% coalescent trees had negligible differences in support values.

Overall, the top two phylogenies are at a 70% matrix completeness threshold, and 50% and 75% informativeness filtering threshold respectively. These two datasets have the same topologies for both maximum likelihood and coalescent analyses, with negligible differences in support values for the maximum likelihood analysis. The 50% informativeness threshold has a slightly higher likelihood. However, in addition to the lower support values in the coalescent

analysis for the 50% top informativeness locus dataset (a decrease in 0.09 posterior probability at the node of *R. reticulata* and the *fantastica* group compared to the 75% informativeness threshold), cutting more informative loci in the 50% informativeness threshold results in a substantial cut of around 15,000 parsimony-informative sites, a very large cut in genetic resources. For these reasons, I decided to simply proceed with interpretation of the original dataset with a 70% matrix completeness and top 75% locus informativeness threshold filtering scheme.

Table 1. Summary statistics for differently filtered datasets. In the dataset column, the number before the dash corresponds to the matrix completeness threshold percentage used, and the number following the dash corresponds to the threshold of locus informativeness used for filtering. Filtering step 1 corresponds to filtering for matrix completeness, and filtering step 2 corresponds to filter for locus informativeness.

Trial Type	Dataset	Loci retained from filtering step 1	Loci retained from filtering step 2	PIS	Log-likelihood
Completeness	50p-top75p	1976	1482	86832	-4.54×10^6
	70p-top75p	1568	1176	72838	-1.57×10^6
	80p-top75p	977	733	46217	-2.37×10^6
	90p-top75p	125	94	5406	-2.94×10^5
Informativeness	70p-top50p	1568	784	59529	-1.21×10^6
	70p-top80p	1568	1254	74773	-1.63×10^6
	70p-top90p	1568	1411	77929	-1.73×10^6
	Normal distribution	1568	1494	68125	-1.60×10^6

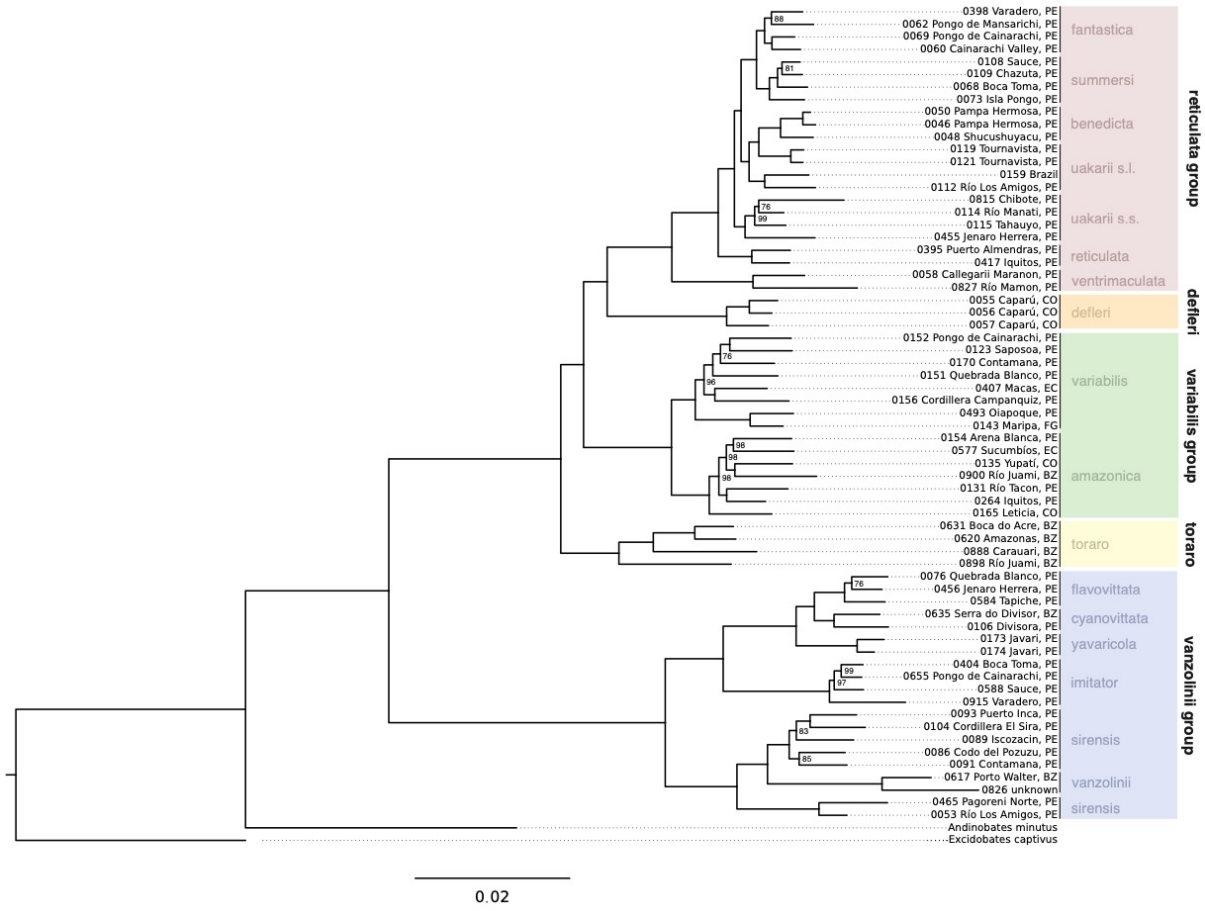

Figure 1. Maximum likelihood tree generated in IQ-TREE. Species groups are highlighted in a common color. Bootstrap values under 100 are included.

Phylogenetic Analyses

My maximum likelihood and coalescent phylogenies were very similar and both had high support values on nodes (Figure 1, Figure 2). Under these results, *R. toraro* and *R. defleri* are no longer sister species. Rather, *R. toraro* is sister to the *variabilis* group, the *reticulata* group, and *R. defleri*, while *R. defleri* remains sister to the *reticulata* group (Figure 1). Thus, *R. toraro* and *R. defleri* constitute two separate species groups, instead of the single *R. defleri* group comprised of *R. toraro* and *R. defleri*. I also found that my eastern *R. amazonica* samples from Maripa,

French Guiana and Pará, Brazil were nested within the *R. variabilis* clade rather than the *R. amazonica* clade. Further, my analysis indicated *R. uakarii* is split into two different groups. One group, composed of species occupying the southern range of the species, are closer related to *R. benedicta*. The other *R. uakarii* populations form a clade sister to the *fantastica* group and these southern *R. uakarii* populations, suggesting *R. uakarii* may actually be two separate species. Lastly, I found that *R. sirensis* was not monophyletic. Instead, one *R. sirensis* population was sister to a clade containing the common ancestor of the remaining *R. sirensis* populations and *R. vanzolinii* (Figure 1). To test each of these topology differences, I generated six constrained topologies to test that were identical to the maximum likelihood tree, each consisting of a single change in topology from the maximum likelihood tree, reflective of topologies found in Brown et al (2011b). The AU topology tests rejected all of the alternative topology hypotheses ($p < 0.05$) (Table S1).

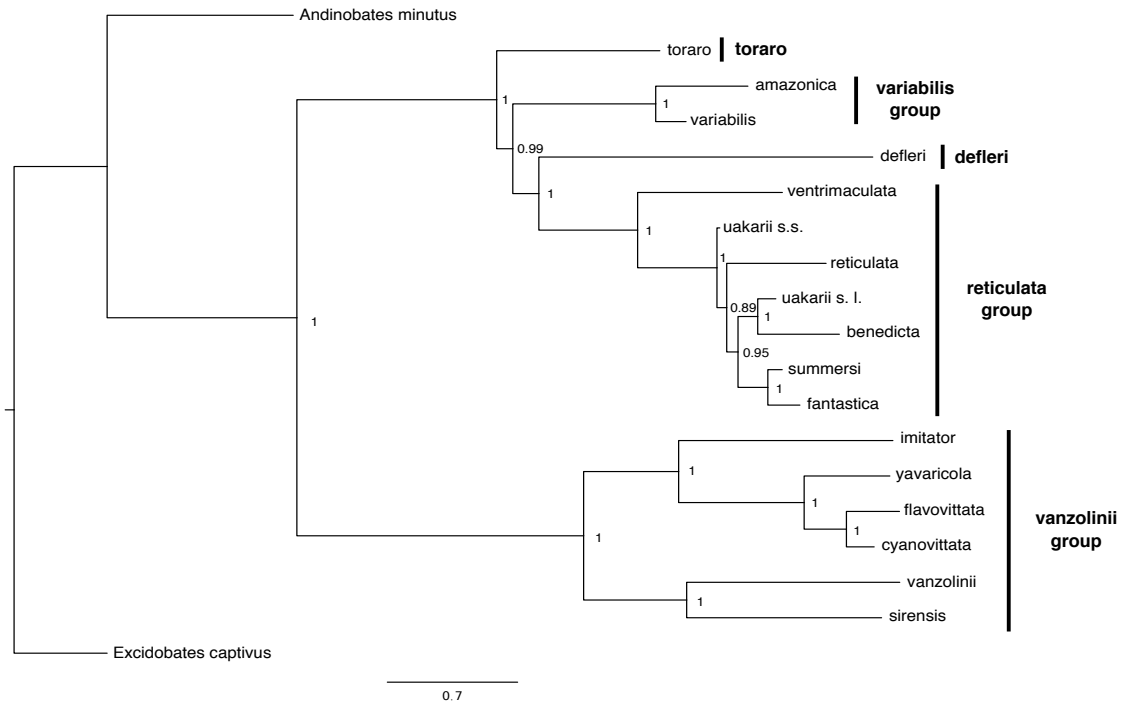

Figure 2. Species-tree generated using ASTRAL-III generated by summarizing gene trees constructed for the 1176 captured loci in the dataset. Support values represent posterior probabilities.

Divergence Time Estimation

The two MCMCTree runs nearly converged. Most nodes had ESS values well above 200 and almost identical mean divergence times at each node. A few older nodes (nodes 1-6) did not have high enough ESS values, yielding greater uncertainty (Figure A1), but still had quite similar node values (Table S3). Results indicate the common ancestor of *Ranitomeya* diverged from sister genus *Andinobates* approximately 11-12 million years ago (Figure 3). Diversification in the group was initially relatively slow, until about 4 to 6 million years ago when lineages began radiating more rapidly into more species, especially in the *reticulata* clade. Error bars increase with deeper time, reflecting greater uncertainty. These divergence time estimations were very similar to *Ranitomeya* divergence times inferred by Guillory et al. (2019) in their analysis on

Dendrobatidae phylogeny. Both my analysis and the analysis done by Guillory et al. (2019) used UCE data and calibration points derived from Santos et al. (2009), making the reasons these similarities arose unclear. This is especially curious because Guillory et al. (2019) used BEAST on the top 200 most informative loci in their analysis for divergence time estimation, compared with my use of my entire dataset in MCMCTree. Overall, my estimates were slightly more recent than estimates found by Santos et al. (2009).

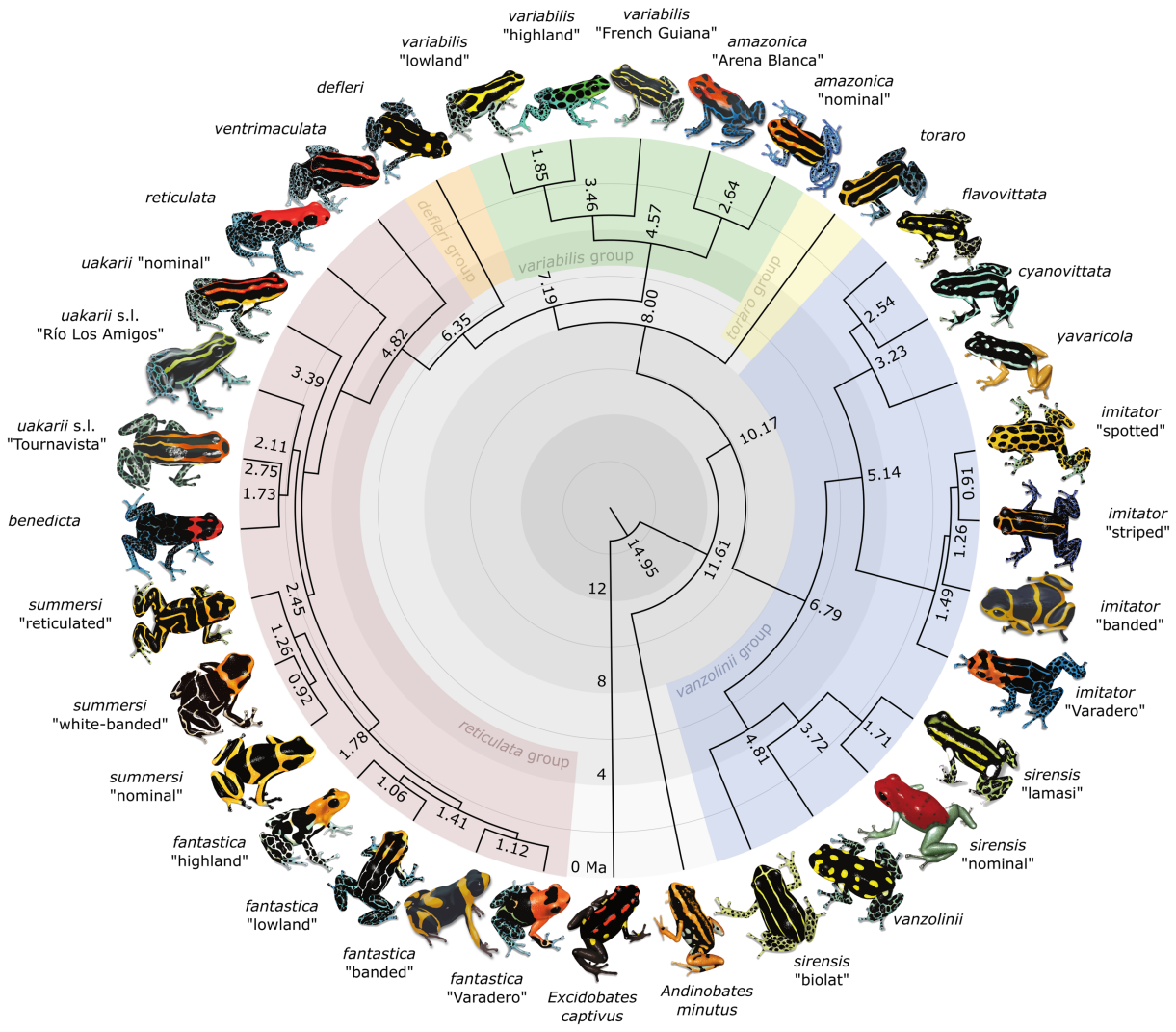

Figure 3. Time-calibrated phylogeny for *Ranitomeya* generated using MCMCTree. Each terminal represents each morph within a species. Time units are in millions of years. Species groups are highlighted and labeled. Frog illustrations for banded *R. imitator*, Arena Blanca *R. amazonica*, eastern *R. variabilis*, *R. uakarii* sensu lato, and banded *R. fantastica* by WXG. All other frog images by Ted Kahn in Kahn et al. (2016). Figure design by WXG.

CHAPTER 4

DISCUSSION

Systematic Implications

The defleri group. Prior to this study, *R. defleri* and *R. toraro* were considered a single species group deemed the *defleri* species group, with commonalities in color pattern featuring a black dorsum with complete or fragmented yellow dorsolateral stripes (Brown et al. 2011b), and similar buzzing, insect-like vocalizations. Both maximum likelihood and coalescent analyses conclusively support that *R. toraro* does not fall sister to *R. defleri*, dismantling the *R. defleri* species group sensu Brown et al. (2011b). Because it was described the most recently of any *Ranitomeya* species and occupies isolated, undisturbed rainforests in Brazilian and Colombian Amazonia (Brown et al. 2011a), *R. toraro* has been less densely sampled than other *Ranitomeya* species. This lack of sampling has likely contributed to the uncertainty of the systematic position of *R. toraro* among different studies. More phylogenomic analysis and taxon sampling of *R. toraro* across its expansive range is necessary to clarify its placement in the *Ranitomeya* phylogeny.

The reticulata group. The *reticulata* group is a monophyletic group consisting of six described species. All species possess vocalizations consisting of a series of very short buzz-like notes (0.1-0.5 sec in length) given in rapid succession (100-200 notes per minute; Brown et al. 2011b). Most members of this group possess red or orange pigmentation concentrated on the head. In general, most relationships are largely consistent with previous phylogenetic and taxonomic studies (Brown et al. 2011b). However, within the *R. fantastica* species complex and *R. uakarii* there are noteworthy differences. First, I consistently recover *R. uakarii* as paraphyletic, with the Nominotypical and Tri-Country morphs (sensu Brown et al. 2011b,

hereafter considered *R. uakarii* sensu strictu) forming one monophyletic group sister to a clade containing the *Ranitomeya fantastica* complex and the *R. uakarii* Toraro morph (sensu Brown et al. 2011b; hereafter considered *R. uakarii* sensu lato). *R. uakarii* sensu lato is nested within the *Ranitomeya fantastica* complex, with Tournavista samples sister to *R. benedicta* and other *R. uakarii* sensu lato sister to both Tournavista samples of *R. uakarii* sensu lato and *R. benedicta*. These results suggest that *R. uakarii* sensu lato may merit specific status, which is supported by the unique phenotypes. The elevation of *R. uakarii* sensu lato as a unique species would improve phylogenetic issues in this group, however, paraphyly in *R. uakarii* (sensu Brown et al. 2011b) would not be entirely reconciled. In this situation, the sister relationship between *R. benedicta* and Tournavista populations of *R. uakarii* sensu lato would still render *R. uakarii* sensu lato paraphyletic. In this case, given the close geographic proximity of these two populations, I suspect that the Tournavista populations sister to *R. benedicta* (which appear most similar to *R. uakarii* sensu strictu) are reflective of historical introgression between the ancestor to *R. benedicta* and *R. uakarii* sensu lato, though rigorous population genetic analyses are required to confirm this prediction.

The phylogenomic results of this study also necessitate redefinition of *Ranitomeya summersi* (Brown et al. 2008, Twomey and Brown 2009). My results match the results of Brown et al. (2011b), where individuals of *R. fantastica* from the Lower Huallaga are nested within *R. summersi*. As discussed by Brown et al. (2011b), it appears these individuals were erroneously ascribed to *R. fantastica.* Based on similar morphology to *R. summersi*, being black with bright-orange dorsal and limb stripping (Figure A2, Figure A3), and my phylogenomic results, I consider these populations members of *R. summersi.* The other population of *R. fantastica* from nearby Tarapoto that is also nested within the *R. summersi* clade is a bit more problematic and

requires further study (increased population-level sampling) and analyses. There is a possibility that poison frog collectors released *R. summersi* in this locality that is near one of the larger cities in the region for easier future collection during the late 1990s and 2000s (personal comm. Rainer Schulte, Pasqual Tafur). This site also likely contained a small native population of *R. fantastica* that was similar in appearance and genetics to nearby localities. No other nearby population (e.g., those from San Antonio or the Cainarachi Valley) possesses the intermediate phenotype (between *R. summersi* and *R. fantastica*) or has been observed to be genetically similar to *R. summersi.* Therefore, reaffirming support for *R. summersi*, *R. benedicta*, and *R. fantastica* is important to verify they are distinct species. In absence of genomic methods, initial population-level classifications were limited, however with increased sampling and genomic-level data, species boundaries can be better clarified.

The variabilis group. The *variabilis* group consists of a monophyletic group containing two species: *R. variabilis* (Zimmerman and Zimmerman 1988) and *R. amazonica* (Schulte 1999). The two species both exhibit a promiscuous mating strategy with male parental care, and have regularly spaced, buzzing vocalizations 0.16-0.44 seconds in length at rate of 24-70 notes per minute (Brown et al. 2011b). Most of my phylogenomic results are consistent with previously recovered relationships (Brown et al. 2011b), with the exception that I found *R. amazonica* samples from French Guiana (sensu Brown et al. 2011b) and the Pará region of Brazil are instead nested within the *R. variabilis* clade. These eastern populations share similar morphologies to striped *R. variabilis* populations found at many sites in the Loreto and San Martín provinces of Peru, including yellow dorsolateral stripes and a lack of reddish pigmentation. Thus, I consider these populations to be members of *R. variabilis*. My two eastern *R. variabilis* genetic samples were recovered as sister to each other (Figure 1), and diverged from the common ancestor of the

other *R. variabilis* populations around 3.3 million years ago (Table S3). This branch length is relatively long compared to time between divergence events of other *R. variabilis* samples (Figure 3), which is likely the result of isolation by distance due to the difference in geography between east and west populations. To further interrogate this novel result, future phylogenomic studies should include more genetic samples of *R. variabilis* populations not represented in this study, such as those found in other parts of Pará and French Guiana. Increased genetic sampling at the population level from localities not represented will give more resolution into how populations separated in geographic space are related.

The vanzolinii group. Phylogenetic relationships of species in the *vanzolinii* group are in flux, and require both more extensive sampling and interrogative analyses into potential patterns of hybrid introgression and population genetic structure before relationships of described species can be definitively resolved. In this analysis, I found *R. sirensis* to be paraphyletic, with one group of samples representing *R. sirensis* sensu strictu and the former *R. lamasi* (sensu Morales 1992) sister to *R. vanzolinii*, and two *R. sirensis* samples representing the former *R. biolat* (sensu Morales 1992) sister to *R. vanzolinii* and the other *R. sirensis* samples (Figure 1). In particular, the long branch separating *R. biolat* from its common ancestor with *R. vanzolinii* and the other *R. sirensis* samples between 3 and 7 million years ago suggests that *R. biolat* could be a legitimate species (Figure A1). However, ongoing studies on *vanzolinii* group systematics using finer taxon sampling and more interrogative bioinformatic methods do not find *R. sirensis* to be paraphyletic, casting skepticism on the validity of my results (Twomey et al. unpub. data). In addition, the other interspecific relationships I found in the *vanzolinii* group were surprising, especially the recovery of *R. vanzolinii* within *R. sirensis*. *R. vanzolinii* has almost always been recovered sister to *R. flavovittata* in previous studies including both species in their taxon

sampling (Roberts et al. 2006, Twomey and Brown 2008, Perez-Peña et al. 2010, Brown et al. 2011b, Grant et al. 2017), whereas *R. sirensis* served as an outgroup to the remainder of the species in the *R. vanzolinii* group. Further genomic studies will be required to address these unexpected results.

Biogeographic implications

The broader understanding of biogeographic history in *Ranitomeya* is improved by my results. The nexus of *Ranitomeya* diversity is in east-central and northeastern Peru, with comparatively little species diversity in the greater Amazon basin (Figure 4), similar to the dendrobatid genus *Ameerega* (Guillory et al. 2020). A principal question is whether the recent and dynamic paleogeographic history of Amazonia contributed to the diversification of *Ranitomeya*, most notably the orogeny of the Andes Mountains. The recent uplift of the Andes in the Late Miocene has long been a suggested principal driver of Neotropical diversification (Hoorn et al. 2010). Santos et al. (2009) found evidence of several dendrobatid migrations from the Andes to the nascent Amazon beginning at 10 million years ago. The orogeny and resulting topographic heterogeneity in the region likely fomented the diversification of *Ranitomeya* and other dendrobatids by generating new local-scale climatic regimes and ecological niches. I dated the divergence between *Ranitomeya* and its sister genus *Andinobates* at about 12 million years ago in this analysis (Figure 3), which corresponds to both Santos et al.'s findings (2009) and to an intense period of uplift in the central Andes (Hoorn et al. 2010).

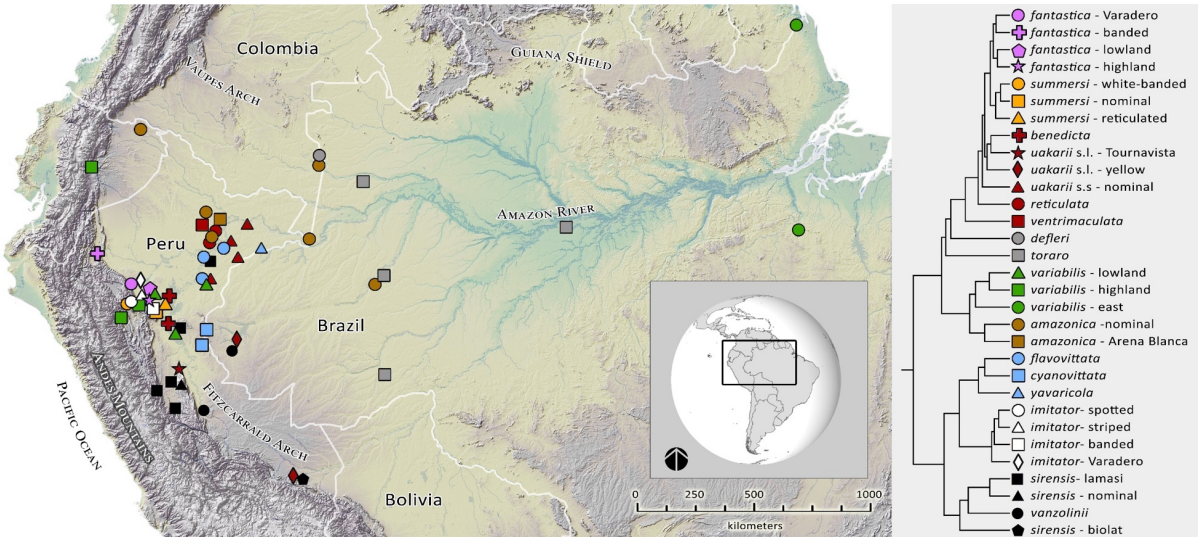

Figure 4. Map of sequenced *Ranitomeya* localities used in the full 67-terminal phylogeny generated in IQ-TREE. The reduced phylogeny sensu Brown et al. (2011b) contains one tip per species morph. Symbols on tips correspond to morph localities on the map. Each species has a common color for all morphs, and different shaped symbols represent different morphs within that color species.

There is also a potential role for Late Miocene marine incursions in the evolution of biogeography in *Ranitomeya*. The "Pebas" megawetland system developed in northwestern Amazonia, in tandem with an intense period of Andean uplift in the Late Miocene (~20-10 Ma) (Hoorn 1993, Hoorn 1994, Wesselingh et al. 2001, Hoorn et al. 2010, Jaramillo et al. 2017, though see Latrubesse et al. 2010), followed by a transition to the fluvial "Acre" system until around 7 million years ago (Hoorn et al. 2010, Latrubesse et al. 2010). This incursion is thought to be responsible for the proliferation of normally marine animals such as dolphins and stingrays in the Amazon (Hoorn et al. 2010), and its potential effects on diversification have been studied in both terrestrial (Chazot et al. 2019) and aquatic (Cooke et al. 2012) taxa. As the megawetland habitat would have been unsuitable for dendrobatid frogs, it is likely that its presence restricted the ancestors of *Ranitomeya* to the Andes and surrounding environs until around 7 million years

ago. Indeed, the *Ranitomeya* species that have made major inroads into greater lowland Amazonia (*R. variabilis, amazonica,* and *toraro*) diverged from their most recent common ancestor around ~6.5 Ma (Figure 3), and repeated marine incursions in northwestern Amazonia have previously been suggested as drivers of repeated vicariance-driven speciation for some dendrobatids (Symula et al. 2003).

A few studies have debated whether the origins of Andean dendrobatids were in the Amazonian highlands in the foothills of the Andes, or in the Amazonian lowlands to the east, mostly in the genus *Ameerega* (Roberts et al. 2006, Brown and Twomey 2009). Brown and Twomey (2009) and Guillory et al. (2020) both suggested an Andean origin for *Ameerega,* and here I propose a similar history for *Ranitomeya.* A principal line of evidence is that the sister genus to *Ranitomeya*, *Andinobates,* is composed of Andean species (Brown et al. 2011b) (members of the genus *Excidobates,* sister to the *Ranitomeya-Andinobates* clade, are also highland taxa). Furthermore, most *Ranitomeya* species occur in the Amazon lining the eastern versant of the Andes, rather than ranging throughout the Amazon Basin (*R. variabilis, amazonica,* and *toraro* are the exceptions). These restricted ranges are also significant for the incredibly labile color pattern evolution in *Ranitomeya*, because many species near the Peruvian Andes exhibit Müllerian mimicry with congeners (e.g., *R. variabilis* and *R. imitator* at Varadero, Peru; Brown et al. 2011b), and model species must colonize areas prior to mimic species before Müllerian mimicry can evolve. Indeed, my divergence time estimates indicate variable morphs of *R. imitator* diversified later in time than sympatric model species *R. variabilis* (Figure 3), potentially indicating that *R. imitator* dispersed from the highlands slower than its congeners. However, sympatric model morphs of *R. fantastica* diverged around the same time as *R. imitator* (Figure 3), indicating that timing of species dispersal may not have contributed to mimicry in this

case. Biogeographic simulations and more investigation into color pattern evolution are necessary to examine this prediction.

My novel recovery of French Guiana and eastern Brazil '*R. amazonica'* individuals as members of *R. variabilis* precludes a simple biogeographic explanation for the eastward radiation of the species, and the mechanisms of this radiation remain poorly resolved and perhaps more complex than previously thought. The two prevalent hypotheses explaining the mechanisms of this eastward radiation are the montane dispersal hypothesis and the riverine-raft hypothesis (Noonan and Wray 2006). Both hypotheses propose dispersal from an Andean ancestor eastward (Brown et al. 2011b, Brown and Twomey pers comm). The first hypothesis proposes that ancestral *Ranitomeya* dispersed throughout the Andes across the Guiana Shield and secondarily into the lower elevation rainforests of eastern Brazil. This could partially explain the relative absence of *Ranitomeya* species in northern Amazonia (e.g., Venezuela) stretching out east, with the exception of the populations in eastern Brazil and French Guiana, possibly suggesting extirpation by climatic events of *Ranitomeya* populations that used to occupy these areas. The second hypothesis, however, proposes that ancestral *Ranitomeya* dispersed via the Amazon on vegetative rafts that are frequently observed during the rainy season floating downstream (Brown and Twomey unpub. data). This second hypothesis appears to be more probable, given the frequency with which very substantive masses of vegetation have been observed, often that including several trees, and at times, considerably large masses of soil (Brown and Twomey pers. comm). This mode of dispersal could also cover thousands of river-kilometers relatively quickly, even in a matter of months (Kozel 2002). Conversely, a montane dispersal via the Andes and Guiana Shield would likely require several hundreds to thousands of years, given that a dispersal of about 2 km could occur with every 1-year generation, resulting in

a full 2,250 years to cover the distance of the approximately 4,500 km chain of mountains that separates currently known distributions of *R. variabilis* in the east from those in the west. This does not, however, discount the possibility of montane dispersal, because *R. variabilis* has a rather disjunct distribution in the Andean foothills, eastern Amazonas and the Guiana Shield. Rather, I suggest that dispersal by riverine-rafting is more likely, given the shorter timescale. Additionally, landslides are more common in the mountains than in the lowlands, suggesting that land rafts would be more likely to form there as a result of landslides. I envision that the earth rafts would also be more likely to landfall in the wider stretches of the Amazon when river currents are reduced. These areas are more abundant near the Amazon river delta in extreme eastern Brazil nearby French Guiana, both of which contain present-day populations of *R. variabilis*.

Though both the montane dispersal and the riverine-raft hypotheses are plausible, each scenario would exhibit markedly different biogeographic signatures. A slow, terrestrial dispersal fitting the montane dispersal hypothesis would lead to genetic structure fitting an isolation-by-distance pattern throughout the Andes and the Guiana Shield. Conversely, a pattern of mixed, poorly structured genetic diversity among the two regions would suggest support for the riverine-raft mode of dispersal, though a more definitive signature of the riverine-raft hypotheses would be downriver populations possessing higher proportions of unique polymorphic sites. There is no specific outstanding genetic evidence suggesting there is more undiscovered diversity (e.g. undiscovered populations where species are currently thought to be absent) in wide-ranging species such as *R. variabilis*. The branch separating eastern *R. variabilis* populations from their western relatives is long, but this could simply be indicative of an early dispersal event (Figure 3). However, more intensive sampling in areas lacking representative specimens could certainly

still reveal undiscovered populations, especially for species such as *R. variabilis* which possess a continental range. Overall, further investigation into genetic structure among populations of wide-ranging *Ranitomeya* species such as *R. variabilis* is required to clarify the biogeographic origins of present-day geographic distributions of *Ranitomeya*.

Future Directions

My time-calibrated genomic phylogeny will open the door to many new studies that were not previously possible in absence of a finely sampled phylogeny. Because the taxa in my phylogeny represent phenotypic diversity across the genus, evolutionary rates derived from the timetree can be used gather insights on whether certain phenotypes evolve faster in others. Ancestral state reconstruction of color phenotypes can also shed further light into color pattern evolution. Further, in tandem with spatial analyses and morph-level ecological niche modeling, insights into rate of phenotype evolution can be transposed to a spatial scale to predict incidences of Müllerian mimicry in geographic space. Revised species relationships open exciting new questions into population genetic relationships for investigation among more complicated species complexes, particularly the *fantastica* complex. Population genetic analyses will reveal more about the evolutionary history among these species, particularly *R. fantastica* and *R. summersi*. Lastly, my insights into biogeographic history of *Ranitomeya* and the novel placement of eastern *R. variabilis* populations spurs the need for interrogative biogeographic analysis that will give broader insight into why some species occupy large ranges and other closely related species remain relatively insular. Overall, this work demonstrates the ability of genome-scale data to uncover new insights in phylogenies of well-studied organisms, and I recommend continued incorporation of phylogenomic insights into evolutionary analyses on *Ranitomeya*.

Concluding Remarks

I address outstanding issues in phylogeny of *Ranitomeya* poison frogs using a diversity of phylogenetic methods on genome-scale data representing comprehensive taxonomic, geographic, and phenotypic diversity. My results indicate that *Ranitomeya* diverged from its sister genus *Andinobates* around 11 million years ago, and began diverging rapidly around 4 to 6 million years ago into several different species groups with much diversity in color pattern. I find that *R. toraro* and *R. defleri* are not sister species, but rather two separate species groups, with *R. defleri* sister to the *reticulata* group and *R. toraro* sister to the clade composed of the *reticulata* group and *R. defleri*. Eastern *R. amazonica* samples in my analysis from French Guiana and northwestern Brazil were recovered within the *R. variabilis* clade, and I reassign those populations to *R. variabilis*. Lastly, *R. uakarii* is split into two clades nested within the *reticulata* group, one representing samples from the northern *R. uakarii* range and the other consisting of samples from the southern *R. uakarii* range. My results, specifically my placement of eastern '*R. amazonica*' populations as *R. variabilis*, indicate that *Ranitomeya* biogeographic history may be more complicated than previously thought. I suggest additional investigation into population genetic structure to resolve whether eastward radiation of *Ranitomeya* is the result of a slow secondary dispersal along the Guiana Shield from the high to low altitudes, or a more rapid dispersal eastward on riverine rafts. I also recommend future studies continue to incorporate genome-scale data into phylogenomic analyses on *Ranitomeya* to continue addressing questions of color pattern evolution and biogeography.

REFERENCES

Bolger, A. M., M. Lohse, and B. Usadel., 2014. Trimmomatic: a flexible trimmer for Illumina sequence data. Bioinformatics 30:2114–2120.

Boulenger G.A. 1883. On a collection of frogs from Yurimaguas, Huallaga River, Northern Peru. Proceedings of the Zoological Society of London 1883:635–638.

Brown, J. L., J. P. Caldwell, E. M. Twomey, P.R. Melo-Sampaio, and M. B. D. Souza. 2011a *Ranitomeya toraro*. Pages 42–47. A taxonomic revision of the Neotropical poison frog genus *Ranitomeya* (Amphibia: Dendrobatidae). Magnolia Press, Auckland, New Zealand.

Brown, J. L., R. Schulte, and K. Summers. 2006. A new species of *Dendrobates* (Anura: Dendrobatidae) from the Amazonian lowlands in Peru. Zootaxa 1152:45–58.

Brown, J. L., and E. M. Twomey. 2009. Complicated histories: three new species of poison frogs of the genus *Ameerega* (Anura: Dendrobatidae) from north-central Peru. Zootaxa 2049:1–38.

Brown, J. L., E. M. Twomey, A. Amézquita, M. B. de Souza, J. P. Caldwell, S. Lötters, R. von May, P. R. Melo-Sampaio, D. Mejía-Vargas, P. Perez-Peña, M. Pepper, E. H. Poelman, M. Sanchez-Rodriguez, and K. Summers. 2011b. A taxonomic revision of the Neotropical poison frog genus *Ranitomeya* (Amphibia: Dendrobatidae). Zootaxa 3083:1–120.

Brown, J. L., E. M. Twomey, M. Pepper, and M. S. Rodriguez. 2008. Revision of the *Ranitomeya fantastica* species complex with description of two new species from Central Peru (Anura: Dendrobatidae). Zootaxa 1823:1–24.

Chazot, N., K. R. Willmott, G. Lamas, A. V. L. Freitas, F. Piron-Prunier, C. F. Arias, J. Mallet, D. L. De-Silva, and M. Elias. 2019. Renewed diversification following Miocene

landscape turnover in a Neotropical butterfly radiation. Global Ecology and Biogeography 28:1118–1132.

Church, S. H., J. F. Ryan, and C. W. Dunn. 2015. Automation and Evaluation of the SOWH Test with SOWHAT. Systematic Biology 64:1048–1058.

Clough, M., and K. Summers. 2000. Phylogenetic systematics and biogeography of the poison frogs: evidence from mitochondrial DNA sequences. Biological Journal of the Linnean Society 70:515–540.

Cooke, G. M., N. L. Chao, and L. B. Beheregaray. 2012. Marine incursions, cryptic species and ecological diversification in Amazonia: the biogeographic history of the croaker genus *Plagioscion* (Sciaenidae). Journal of Biogeography 39:724–738.

Crothers L. R., and M. E. Cummings. 2013. Warning signal brightness variation: sexual selection may work under the radar of natural selection in populations of a polytypic poison frog. The American Naturalist 181:E116–E124.

Daly J. W., and C. W. Myers. 1967. Toxicity of Panamanian poison frogs (*Dendrobates*): some biological and chemical aspects. Science 156:970–973.

Darst, C. R., and D. C. Cannatella. 2004. Novel relationships among hyloid frogs inferred from 12S and 16S mitochondrial DNA sequences. Molecular Phylogenetics and Evolution 31:462–475.

Edgar, R.C. 2004. MUSCLE: multiple sequence alignment with high accuracy and high throughput. Nucleic Acids Resources 32:1792–1797.

Enciso-Romero J., C. Pardo-Díaz, S. H. Martin, C. F. Arias, M. Linares, W. O. McMillan, C. D. Jiggins, and C. Salazar. 2017. Evolution of novel mimicry rings facilitated by adaptive introgression in tropical butterflies. Molecular Ecology 26:5160–5172.

Faircloth, B.C. 2016. PHYLUCE is a software package for the analysis of conserved genomic loci. Bioinformatics 32:786–788.

Faircloth, B.C. 2013. Illumiprocessor: A Trimmomatic wrapper for parallel adapter and quality trimming. Release 2.0.6. Faircloth Lab, Baton Rouge, Louisiana, USA.

Faircloth, B.C., J. E. McCormack, N. G. Crawford, M. G. Harvey, R. T. Brumfield, and T. C. Glenn. 2012. Ultraconserved elements anchor thousands of genetic markers spanning multiple evolutionary timescales. Systematic Biology 61:717–726.

Goldman, N., J. P. Anderson, and A. G. Rodrigo. 2000. Likelihood-based tests of topologies in phylogenetics. Systematic Biology 49:652–670.

Grabherr, M. G., B. J. Haas, M. Yassour, J. Z. Levin, D. A. Thompson, I. Amit, X. Adiconis, L. Fan, R. Raychowdhury, Q. Zeng, Z. Chen, E. Mauceli, N. Hacohen, A. Gnirke, N. Rhind, F. di Palma, B. W. Birren, C. Nusbaum, K. Lindblad-Toh, N. Friedman, and A. Regev. 2011. Full-length transcriptome assembly from RNA-Seq data without a reference genome. Nature Biotechnology 29:644–652.

Grant, T., D. R. Frost, J. P. Caldwell, R. Gagliardo, C. F. B. Haddad, P. J. R. Kok, D. B. Means, B. P. Noonan, W. E. Schargel, and W. C. Wheeler. 2006. Phylogenetic systematics of dart-poison frogs and their relatives (Amphibia: Athesphatanura: Dendrobatidae). Bulletin of the American Museum of Natural History 299:1–262.

Grant, T., M. Rada, M. Anganoy-Criollo, A. Batista, P. H. Dias, A. M. Jeckel, D. J. Machado, and J. V. Rueda-Almonacid. 2017. Phylogenetic systematics of dart-poison frogs and their relatives revisited (Anura: Dendrobatoidea). South American Journal of Herpetology 12:S1–S90.

Guillory, W. X., C. M. French, E. M. Twomey, G. Chávez, I. Prates, R. von May, I. De la Riva, S. Lötters, S. Reichle, S. J. Serrano-Rojas, A. Whitworth, and J. L. Brown. 2020. Phylogenetic relationships and systematics of the Amazonian poison frog genus *Ameerega* using ultraconserved genomic elements. Molecular Phylogenetics and Evolution 142:106638.

Guillory, W. X., M. R. Muell, K. Summers, and J. L. Brown. 2019. Phylogenomic reconstruction of the Neotropical poison frogs (Dendrobatidae) and their conservation. Diversity 11:126.

Heibl, C. 2008. PHYLOCH: R language tree plotting tools and interfaces to diverse phylogenetic software packages. Release 1.5-5.

Hoorn, C. 1994. An environmental reconstruction of the palaeo-Amazon River system (Middle–Late Miocene, NW Amazonia). Palaeogeography, Palaeoclimatology, Palaeoecology. 112:187–238.

Hoorn, C. 1993. Marine incursions and the influence of Andean tectonics on the Miocene depositional history of northwestern Amazonia: results of a palynostratigraphic study. Palaeogeography, Palaeoclimatology, Palaeoecology. 105:267–309.

Hoorn, C., F. P. Wesselingh, H. ter Steege, M. A. Bermudez, A. Mora, J. Sevink, I. Sanmartin, A. Sanchez-Meseguer, C. L. Anderson, J. P. Figueiredo, C. Jaramillo, D. Riff, F. R. Negri, H. Hooghiemstra, J. Lundberg, T. Stadler, T. Sarkinen, and A. Antonelli. 2010. Amazonia through time: Andean uplift, climate change, landscape evolution, and biodiversity. Science 330:927–931.

Hosner, P.A., B. C. Faircloth, T. C. Glenn, E. L. Braun, and R. T. Kimball. 2016. Avoiding missing data biases in phylogenomic inference: an empirical study in the landfowl (Aves: Galliformes). Molecular Biology and Evolution. 33:1110–1125.

Jaramillo, C., I. Romero, C. D'Apolito, G. Bayona, E. Duarte, S. Louwye, J. Escobar, J. Luque, J. D. Carrillo-Briceño, V. Zapata, A. Mora, S. Schouten, M. Zavada, G. Harrington, J. Ortiz, F. P. Wesselingh. 2017. Miocene flooding events of western Amazonia. Science Advances 3:e1601693.

Jiggins C. D. Ecological speciation in mimetic butterflies. 2008. BioScience 58:541–548.

Kahn, T. R., E. La Marca, S. Lötters, J. L. Brown, E. M. Twomey, and A. Amézquita. 2016. Aposematic poison frogs (Dendrobatidae) of the Andean countries: Bolivia, Colombia, Ecuador, Perú, and Venezuela. First edition. Conservation International, Arlington, USA.

Kalyaanamoorthy, S., B. Q. Minh, T. K. F. Wong, A. von Haeseler, and L. S. Jermiin. 2017. ModelFinder: fast model selection for accurate phylogenetic estimates. Nature Methods 14:587–589.

Kishino, H., and M. Hasegawa. 1989. Evaluation of the maximum likelihood estimate of the evolutionary tree topologies from DNA sequence data, and the branching order in Hominoidea. Journal of Molecular Evolution 29:170–179.

Kozel, B. 2002. Three men in a raft: an improbable journey down the Amazon. First edition. Pan Macmillan Australia, Sydney, Australia.

Latrubesse, E. M., M. Cozzuol, S. A. F. da Silva-Caminha, C. A. Rigsby, M. L. Absy, and C. Jaramillo. 2010. The Late Miocene paleogeography of the Amazon Basin and the evolution of the Amazon River system. Earth-Science Reviews 99:99–124.

Lawrence J. P., B. Rojas, A. Fouquet, J. Mappes, A. Blanchette, R. A. Saporito, R. J. Bosque, E. A. Courtois, and B. P. Noonan. 2019. Weak warning signals can persist in the absence of gene flow. Proceedings of the National Academy of Sciences, 116:19037–19045.

Mallet J., and M. Joron. 1999. Evolution of diversity in warning color and mimicry: polymorphisms, shifting balance, and speciation. Annual Review of Ecology and Systematics 30:201–233.

Morales, V. 1992. Dos especies nuevas de *Dendrobates* (Anura: Dendrobatidae) para Perú. Caribbean Journal of Science. 28:191–199.

Myers C. W. 1982. Spotted poison frogs: Descriptions of three new *Dendrobates* from Western Amazonia, and resurrection of a lost species from "Chiriqui." American Museum Novitates 2721:1–23.

Myers, C. W., and J. W. Daly. 1980. Taxonomy and ecology of *Dendrobates bombetes*, a new Andean poison frog with new skin toxins. American Museum Novitates, 1–23.

Nguyen, L. T., H A. Schmidt, A. von Haeseler, and B. Q. Minh. 2015. IQ-TREE: A fast and effective stochastic algorithm for estimating maximum-likelihood phylogenies. Molecular Biology and Evolution 32:268–274.

Noonan, B. P., and K. P. Wray. 2006. Neotropical diversification: the effects of a complex history on diversity within the poison frog genus *Dendrobates*. Journal of Biogeography 33:1007–1020.

Perez-Peña, P. E., G. Chavez, E. M. Twomey, and J. L. Brown. 2010. Two new species of *Ranitomeya* (Anura: Dendrobatidae) from eastern Amazonian Peru. Zootaxa 2439:1–23.

Persons, N. W., P. A. Hosner, K. A. Meiklejohn, E. L. Braun, and R. T. Kimball. 2016. Sorting out relationships among the grouse and ptarmigan using intron, mitochondrial, and ultra-conserved element sequences. Molecular Phylogenetics and Evolution. 98:123–132.

Pyron, R. A., and J. J. Wiens. 2011. A large-scale phylogeny of Amphibia including over 2800 species, and a revised classification of extant frogs, salamanders, and caecilians. Molecular Phylogenetics and Evolution. 61:543–583.

R Core Team. 2015. R: a language and environment for statistical computing. Release 3.2.3. The R Foundation for Statistical Computing, Vienna, Austria.

Rambaut, A., A. J. Drummond, D. Xie, G. Baele, and M. A. Suchard. 2018. Posterior summarization in Bayesian phylogenetics using Tracer 1.7. Systematic Biology 67:901–904.

Roberts, J. L., J. L. Brown, R. von May, W. Arizabal, R. Schulte, and K. Summers. 2006. Genetic divergence and speciation in lowland and montane Peruvian poison frogs. Molecular Phylogenetics and Evolution 41:149–164.

Santos, J. C., L. A. Coloma, and D. C. Cannatella. 2003. Multiple, recurring origins of aposematism and diet specialization in poison frogs. Proceedings of the National Academy of Science 100:12792–12797.

Santos, J. C., L. A. Coloma, K. Summers, J. P. Caldwell, R. Ree, and D. C. Cannatella. 2009. Amazonian amphibian diversity is primarily derived from Late Miocene Andean lineages. PLoS Biology 7:e1000056.

Savage J. M. 2002. The Amphibians and Reptiles of Costa Rica: a herpetofauna between two continents, between two seas. First edition. The University of Chicago Press, Chicago, Illinois, USA.

Silverstone P. A. 1975. A revision of the poison-arrow frogs of the genus *Dendrobates* Wagler. Natural History Museum of Los Angeles County 21:1–55.

Schulte R., 1999. Pfeilgiftfrösche “Artenteil - Peru”. First edition. INBICO, Wailblingen, Germany.

Shimodaira, H. 2002. An approximately unbiased test of phylogenetic tree selection. Systematic Biology 51:492–508.

Streicher, J. W., and J. J. Wiens. 2017. Phylogenomic analyses of more than 4000 nuclear loci resolve the origin of snakes among lizard families. Biology Letters 13:20170393.

Strimmer, K., and A. Rambaut. 2002. Inferring confidence sets of possibly misspecified gene trees. Proceedings of the Royal Society London B 269:137–142.

Summers, K., E. Bermingham, L. Weigt, S. McCafferty, and L. Dahistrom. 1997. Phenotypic and genetic divergence in three species of dart-poison frogs with contrasting parental behavior. Journal of Heredity 88:8–13.

Summers, K., T. W. Cronin, and T. Kennedy. 2003. Variation in spectral reflectance among populations of *Dendrobates pumilio*, the strawberry poison frog, in the Bocas del Toro Archipelago, Panama. Journal of Biogeography 30:35–53.

Summers, K., L. A. Weigt, P. Boag, and E. Bermingham. 1999. The evolution of female parental care in poison frogs of the genus *Dendrobates*: evidence from mitochondrial DNA sequences. Herpetologica 55:254–270.

Symula, R., R. Schulte, and K. Summers. 2003. Molecular systematics and phylogeography of Amazonian poison frogs of the genus *Dendrobates*. Molecular Phylogenetics and Evolution 26:452–475.

Symula, R., R. Schulte, and K. Summers. 2001. Molecular phylogenetic evidence for a mimetic radiation in Peruvian poison frogs supports a Müllerian mimicry hypothesis. Proceeds of the Royal Society London B Biological Sciences 268:2415–2421.

Twomey, E. M., and J. L. Brown. 2008. Spotted poison frogs: rediscovery of a lost species and a new genus (Anura: Dendrobatidae) from northwestern Peru. Herpetologica 64:121–137.

Twomey, E. M., and J. L. Brown. 2009. Another new species of *Ranitomeya* (Anura: Dendrobatidae) from Amazonian Colombia. Zootaxa 2302:48–60.

Twomey, E. M., J. S. Vestergaard, P. J. Venegas, and K. Summers. 2016. Mimetic divergence and the speciation continuum in the mimic poison frog (*Ranitomeya imitator*). The American Naturalist 187:205–224.

Vences, M., J. Kosuch, S. Lötters, A. Widmer, K. H. Jungfer, J. Köhler, and M. Veith. 2000. Phylogeny and classification of poison frogs (Amphibia: Dendrobatidae), based on mitochondrial 16S and 12S ribosomal RNA gene sequences. Molecular Phylogenetics and Evolution 15:34–40.

Wang I. J., and K. Summers. 2010. Genetic structure is correlated with phenotypic divergence rather than geographic isolation in the highly polymorphic strawberry poison-dart frog. Molecular Ecology 19:447–458.

Wesselingh, F. P., M. E. Räsänen, G. Irion, H. B. Vonhof, R. Kaandorp, W. Renema, L. Romero Pittman, and M. Gingras. 2001. Lake Pebas: a palaeoecological reconstruction of a Miocene, long-lived lake complex in western Amazonia. Cainozoic Resources 1:35–81.

Wollenberg, K. C., M. Veith, B. P. Noonan, and S. Lötters. 2006. Polymorphism versus species richness—systematics of large *Dendrobates* from the Eastern Guiana Shield (Amphibia: Dendrobatidae). Copeia 2000:623–629.

Yang, Z. 2007. PAML 4: Phylogenetic Analysis by Maximum Likelihood. Molecular Biology and Evolution 24:1586–1591.

Zhang, C., M. Rabiee, E. Sayyari, and S. Mirarab. 2018. ASTRAL-III: polynomial time species tree reconstruction from partially resolved gene trees. BMC Bioinformatics 19:153.

Zimmerman, H., and E. Zimmerman. 1988. Etho-Taxonomie und zoogeographische Artengruppenbildung bei Pfeilgiftfroschen (Anura: Dendrobatidae). Salamandra 24:125–160.

APPENDIX A

SUPPLEMENTAL FIGURES

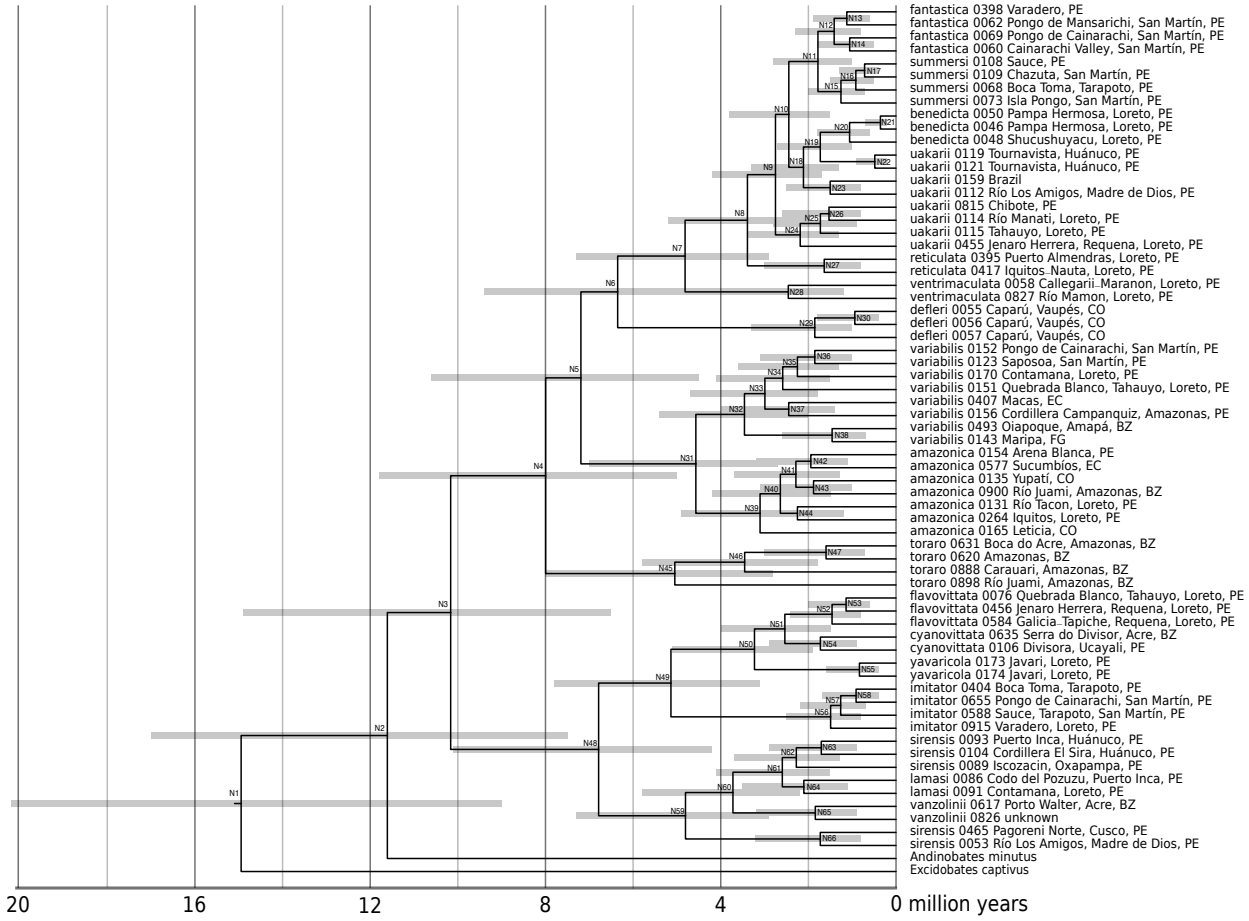

Figure A1. Time-calibrated phylogeny for full 67-terminal phylogeny generated using MCMCTree. Error bars represent bounds of 95% confidence intervals for each node, and time units are in millions of years. Each node label corresponds to divergence times with 95% confidence intervals written in Table S3.

Figure A2. *Ranitomeya* Plate 1. A–P: *Ranitomeya variabilis.* A: Varadero, Loreto, Peru; B: Lower Huallaga Canyon, San Martin, Peru; C: Yupati, Vaupés, Colombia; D: Contamana, Loreto, Peru; E: Shamboyacu, San Martin, Peru; F-G: Upper Cainarachi Valley, San Martin, Peru; H: Saposoa, San Martin, Peru; I: Borja, Loreto, Peru; J: Macas, Morona-Santiago, Ecuador; K: Macuma, Morona-Santiago, Ecuador (J. Verkade), L: Puyo, Pastaza, Ecuador (J. Verkade); M: Archidona, Napo, Ecuador (J. Verkade); N & O: Nouragues, French Guiana (E. H. Poelman); P: French Guiana (B.P. Noonan). Q–V: *Ranitomeya amazonica.* Q. Iquitos, Loreto, Peru; R–T: 'Arena Blanca', Loreto, Peru; U: Upper Rio Mazan-Pintuyacu, Loreto, Peru (J. J. Lopez-Rojas); V. Iquitos, Loreto, Peru (T. Ostrowski). W–X: *Ranitomeya benedicta.* W: Shucushuyacu, Loreto, Peru; X: Pampa Hermosa, Loreto, Peru. Y–BB: *Ranitomeya fantastica.*

Y: near Yumbatos, San Martin, Peru; Z: Varadero, Loreto, Peru; AA: Pongo de Cainarachi, San Martin; BB: Upper Cainarachi Valley, San Martin, Peru. All photos without explicitly stated credit taken by JL Brown and E Twomey.

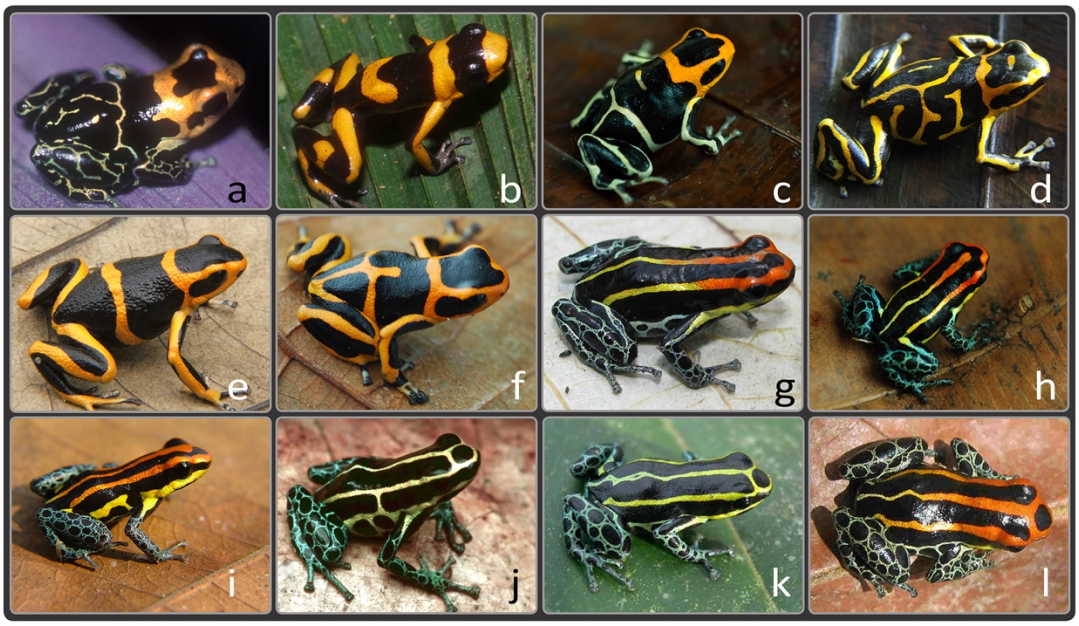

Figure A3. *Ranitomeya* Plate 2. A–B: *Ranitomeya fantastica.* A: San Antonio, San Martin, Peru (K. Summers); B: Santa María de Nieva, Loreto, Peru (K.H. Jungfer); C–F: *Ranitomeya summersi.* C: Tarapoto, San Martin, Peru; D: Lower Huallaga Canyon, San Martin; E: Chazuta, San Martin, Peru; F: Sauce, San Martin, Peru. G–I: *Ranitomeya uakarii* sensu strictu. G: Rio Boncuya, Loreto, Peru (G. Gagliardi); H: Tamshiyacu village, Loreto, Peru; I: Quebrada Blanco, Loreto, Peru; J–L: *Ranitomeya uakarii* sensu lato. J: Rio Los Amigos, Madre de Dios, Peru (Rudolf von May); K: Porto Walter, Acre, Brazil (Janalee Caldwell); L: Tournavista, Huánuco, Peru (A. Toebe). All photos without explicitly stated credit taken by JL Brown and E Twomey.

APPENDIX B

SUPPLEMENTAL TABLES

Table A1. AU topology testing results against maximum likelihood phylogeny. The left-most column contains alternatively tested topologies sensu Brown et al. (2011b), each of which contain single modifications from the maximum likelihood topology as follows: A) eastern *R. variabilis* populations restricted to *R. amazonica* clade, B) *R. summersi* samples from Isla Pongo and Tarapoto restricted to *R. fantastica* clade, C) *R. sirensis* restricted to a monophyletic group, D) *R. toraro* and *R. defleri* restricted to a monophyletic clade sister to the *reticulata* group, E) all *R. uakarii* populations restricted to a monophyletic group, and F) all *R. uakarii* sensu lato populations restricted to a monophyletic group sister to *R. benedicta*. The second column illustrates the difference in log-likelihood value between the maximum likelihood tree and subsequent trees, and bp-RELL refers to bootstrap proportion using the RELL method.

Topology	deltaL	bp-RELL	p-value
Maximum likelihood	0	0.9943	0.9942
A	171	0.0056	0.0079
B	715	0.0000	0.0000
C	343	0.0000	0.0002
D	185	0.0000	0.0001
E	680	0.0000	0.0000
F	256	0.0000	0.0002

Table A2. List of genetic samples used in phylogenetic analyses.

Genus	Species	Latitude	Longitude	Locality	Seq ID	Number of loci
Ranitomeya	*amazonica*	-1.2972	-69.6269	Colombia: Yupatí: near La Pedrera	0135	1852
Ranitomeya	*amazonica*	-1.9639	-67.93528	Brazil: Amazonas: Río Juami	0900	1938
Ranitomeya	*amazonica*	0.00000	-76.16700	Ecuador: Sucumbíos Province	0577	1794
Ranitomeya	*amazonica*	unknown	unknown	Peru: 'Arena Blanca'	0154	1915
Ranitomeya	*amazonica*	-4.024	-73.55	Peru: Loreto: Río Tacon	0131	1844
Ranitomeya	*amazonica*	-1.2972	-69.6269	Peru: Loreto: Iquitos	0264	1622
Ranitomeya	*amazonica*	-4.11228	-69.93964	Colombia: Amazonas: Leticia	0165	1649
Ranitomeya	*variabilis*	-6.29592	-76.23327	Peru: San Martín: Pongo de Cainarachi	0152	1572
Ranitomeya	*variabilis*	-6.922417	-76.8564	Peru: San Martín: Saposoa	0123	1476
Ranitomeya	*variabilis*	-7.259	-74.995	Peru: Loreto: Contamana	0170	1589
Ranitomeya	*variabilis*	-4.358417	-73.184	Peru: Tahauyo: Quebrada Blanco	0151	1774
Ranitomeya	*variabilis*	-1.483	-77.983	Ecuador: Morona-Santiago: Macas	0407	1793
Ranitomeya	*variabilis*	-4.42767	-77.52502	Peru: Amazonas: Cordillera Campanquiz	0156	1704
Ranitomeya	*variabilis*	-3.85972	-51.761	Brazil: Amapa: Oiapoque	0493	1743

Table A2. Continued.

Ranitomeya	*variabilis*	3.814	-51.885	French Guiana: Maripa	0143	1934
Ranitomeya	*fantastica*	-6.295917	-76.233266	Peru: San Martín: Pongo de Cainarachi	0069	1610
Ranitomeya	*fantastica*	-6.42717	-76.2908	Peru: San Martín: Cainarachi Valley	0060	1450
Ranitomeya	*fantastica*	-5.85417	-76.54313889	Peru: Loreto: Varadero	0398	1742
Ranitomeya	*fantastica*	-4.58	-77.9	Peru: Amazonas: Pongo de Mansarichi	0062	1780
Ranitomeya	*summersi*	-6.454667	-76.348847	Peru: San Martín: Tarapoto: Boca Toma	0068	1668
Ranitomeya	*summersi*	-6.726631	-76.222691	Peru: San Martín: Sauce	0108	1238
Ranitomeya	*summersi*	-6.537225	-76.13006	Peru: San Martín: Chazuta	0109	1216
Ranitomeya	*summersi*	-6.43730578	-75.88468027	Peru: San Martín: Isla Pongo	0073	1820
Ranitomeya	*benedicta*	-7.207381	-75.32364	Peru: Loreto: Contamana: Pampa Hermosa	050	1759
Ranitomeya	*benedicta*	-7.207381	-75.32364	Peru: Loreto: Contamana: Pampa Hermosa	0046	2008
Ranitomeya	*benedicta*	-6.032094	-75.856995	Peru: Loreto: Shucushuyacu	0048	1086
Ranitomeya	*uakarii*	-8.948222	-74.767833	Peru: Huánuco: Tournavista	0119	1864
Ranitomeya	*uakarii*	-8.948222	-74.767833	Peru: Huánuco: Tournavista	0121	1292
Ranitomeya	*uakarii*	unknown	unknown	Brazil	0159	1657

Table A2. Continued.

Ranitomeya	*uakarii*	-12.56861	-70.09917	Peru: Madre de Dios: Río Los Amigos	0112	1874
Ranitomeya	*uakarii*	-4.358417	-73.184444	Peru: Loreto: Tahauyo	0115	1316
Ranitomeya	*uakarii*	-3.65201	-72.20045	Peru: Loreto: Río Manati	0114	674
Ranitomeya	*uakarii*	unknown	unknown	Peru: Chibote	0815	1821
Ranitomeya	*uakarii*	-4.90389	-73.6681	Peru: Loreto: Requena: Jenaro Herrera	0455	1683
Ranitomeya	*reticulata*	-3.83077	-73.37327	Peru: Loreto: Puerto Almendras	0395	1706
Ranitomeya	*reticulata*	-4.203	-73.4796	Peru: Loreto: Hacienda Zamora, Iquitos-Nauta	0417	1894
Ranitomeya	*ventrimaculata*	-3.84	-73.62	Peru: Loreto: Callegarii Maranon	0058	1493
Ranitomeya	*ventrimaculata*	unknown	unknown	Peru: Loreto: Río Mamon	0827	1908
Ranitomeya	*defleri*	-1.077072	-69.514261	Colombia: Vaupés: Caparú	0055	2048
Ranitomeya	*defleri*	-1.077072	-69.514261	Colombia: Vaupés: Caparú	0056	1885
Ranitomeya	*defleri*	-1.077072	-69.514261	Colombia: Vaupés: Caparú	0057	1701
Ranitomeya	*toraro*	-9.009161973	-67.18487598	Brazil: Amazonas: Boca do Acre	0631	1590
Ranitomeya	*toraro*	-3.6196	-60.4551	Brazil: Amazonas	0620	1613
Ranitomeya	*toraro*	-5.36028	-67.19861	Brazil: Amazonas: Carauari	0888	1863

Table A2. Continued.

Ranitomeya	*toraro*	-1.96194	-67.93472	Brazil: Amazonas: Río Juami	0898	1864
Ranitomeya	*cyanovittata*	-7.434021989	-73.66021704	Brazil: Acre: Serra do Divisor	0635	1936
Ranitomeya	*cyanovittata*	-7.98	-73.846111	Peru: Ucayali: Divsora	0106	1761
Ranitomeya	*flavovittata*	-5.467377778	-73.93447222	Peru: Loreto: Requena	0584	1834
Ranitomeya	*flavovittata*	-4.358417	-73.184444	Peru: Loreto: Tahauyo: Quebrada Blanco	0076	1559
Ranitomeya	*flavovittata*	-4.90389	-73.6681	Peru: Loreto: Requena: Jenaro Herrera	0456	1750
Ranitomeya	*yavaricola*	-4.45972	-71.750972	Peru: Loreto: Javari	0174	1300
Ranitomeya	*yavaricola*	-4.45972	-71.750972	Peru: Loreto: Javari	0173	1241
Ranitomeya	*imitator*	-6.454667	-76.348847	Peru: San Martín: Tarapoto: Boca Toma	0404	1927
Ranitomeya	*imitator*	-6.29592	-76.23327	Peru: San Martín: Pongo de Cainarachi	0655	1938
Ranitomeya	*imitator*	-6.691470707	-76.21234659	Peru: San Martín: Tarapoto	0588	1729
Ranitomeya	*imitator*	unknown	unknown	Peru: Loreto: Varadero	0915	1707
Ranitomeya	*sirensis*	-9.463583	-74.817472	Peru: Huánuco: Cordillera El Sira	0104	1704
Ranitomeya	*sirensis*	-9.36716	-74.93792	Peru: Huánuco: Puerto Inca	0093	1631
Ranitomeya	*sirensis*	-10.358244	-74.88322	Peru: Pasco: Oxapampa: Iscozacin	0089	1416

Table A2. Continued.

Ranitomeya	*sirensis*	-9.734875	-75.510364	Peru: Huánuco: Codo del Pozuzu	0086	1328
Ranitomeya	*sirensis*	-7.259	-74.995	Peru: Loreto: Contamana	0091	1393
Ranitomeya	*sirensis*	-12.567	-70.1	Peru: Madre de Dios: Río Los Amigos	0053	1287
Ranitomeya	*sirensis*	-4.90389	-73.6681	Peru: Loreto: Requena: Jenaro Herrera	0465	1723
Ranitomeya	*vanzolinii*	-8.25867	-72.77697	Brazil: Acre	0617	1871
Ranitomeya	*vanzolinii*	unknown	unknown	unknown	0826	1958
Andinobates	*minutus*	unknown	unknown	unknown	0244	1560
Excidobates	*captivus*	-4.446704	-77.643595	Peru: Amazonas: Santiago Valley	0239	1936

Table A3. Divergence time estimation values and values of confidence interval bounds. Node numbers correspond to Figure S1. Units are in millions of years.

	MCMCTree Run 1			MCMCTree Run 2		
Node	Mean Posterior Height	Upper 95%	Lower 95%	Mean Posterior Height	Upper 95%	Lower 95%
1	14.95	20.23	9.02	14.10	19.90	8.19
2	11.62	16.99	7.53	12.22	17.57	7.57
3	10.17	14.87	6.53	10.72	15.53	6.57

Table A3. Continued.

4	8.00	11.78	5.04	8.38	12.42	5.00
5	7.20	10.63	4.50	7.53	11.18	4.47
6	6.36	9.44	3.94	6.63	9.97	3.90
7	4.82	7.33	2.91	5.05	7.76	2.91
8	3.39	5.21	2.03	3.59	5.59	2.04
9	2.75	4.21	1.66	2.92	4.55	1.66
10	2.45	3.76	1.46	2.60	4.05	1.47
11	1.78	2.81	1.04	1.89	3.01	1.05
12	1.41	2.28	0.80	1.50	2.44	0.81
13	1.12	1.88	0.60	1.19	2.02	0.61
14	1.06	1.80	0.54	1.12	1.94	0.55
15	1.26	2.03	0.71	1.33	2.20	0.71
16	0.92	1.53	0.49	0.97	1.66	0.50
17	0.72	1.27	0.36	0.76	1.37	0.36
18	2.12	3.27	1.25	2.24	3.52	1.26

Table A3. Continued.

19	1.73	2.72	1.00	1.83	2.94	1.01
20	1.06	1.80	0.56	1.12	1.92	0.57
21	0.36	0.68	0.17	0.38	0.73	0.17
22	0.48	0.94	0.22	0.51	0.99	0.22
23	1.50	2.47	0.81	1.60	2.68	0.82
24	2.19	3.43	1.26	2.32	3.72	1.27
25	1.73	2.82	0.94	1.82	3.03	0.96
26	1.53	2.56	0.80	1.62	2.73	0.81
27	1.64	2.99	0.76	1.75	3.27	0.77
28	2.46	4.25	1.23	2.56	4.51	1.23
29	1.85	3.26	0.95	1.97	3.52	0.97
30	0.94	1.76	0.43	1.00	1.91	0.45
31	4.57	7.00	2.74	4.81	7.46	2.73
32	3.46	5.36	2.04	3.64	5.77	2.03
33	2.99	4.69	1.75	3.14	5.00	1.75

Table A3. Continued.

34	2.59	4.10	1.48	2.71	4.38	1.48
35	2.25	3.61	1.26	2.36	3.87	1.26
36	1.86	3.08	0.98	1.94	3.27	0.99
37	2.45	3.97	1.36	2.57	4.23	1.36
38	1.46	2.64	0.69	1.54	2.87	0.70
39	3.10	4.87	1.81	3.27	5.21	1.80
40	2.64	4.17	1.53	2.78	4.48	1.52
41	2.29	3.66	1.29	2.40	3.91	1.30
42	1.95	3.18	1.06	2.04	3.41	1.06
43	1.88	3.11	1.02	1.97	3.31	1.02
44	2.25	3.66	1.24	2.36	3.93	1.25
45	5.05	8.02	2.76	5.28	8.60	2.83
46	3.46	5.80	1.79	3.61	6.20	1.83
47	1.60	2.99	1.19	1.67	3.20	0.74
48	6.79	10.13	4.25	7.53	11.32	4.46

Table A3. Continued.

49	5.14	7.81	3.10	5.64	8.71	3.22
50	3.23	5.07	1.88	3.49	5.61	1.92
51	2.54	4.04	1.46	2.73	4.44	1.47
52	1.46	2.43	0.79	1.57	2.70	0.79
53	1.14	1.98	0.57	1.22	2.20	0.59
54	1.73	2.95	0.89	1.86	3.25	0.91
55	0.84	1.62	0.37	0.89	1.76	0.38
56	1.49	2.50	0.81	1.59	2.71	0.81
57	1.26	2.17	0.67	1.34	2.34	0.67
58	0.91	1.66	0.43	0.97	1.81	0.44
59	4.81	7.32	2.89	5.29	8.28	2.99
60	3.72	5.76	2.19	4.07	6.45	2.25
61	2.59	4.14	1.48	2.80	4.58	1.51
62	2.28	3.69	1.27	2.46	4.07	1.29
63	1.71	2.91	0.87	1.84	3.22	0.90

Table A3. Continued.

64	2.10	3.49	1.12	2.27	3.87	1.14
65	1.84	3.17	0.94	1.96	3.42	0.97
66	1.73	3.17	0.80	1.85	3.51	0.82

VITA

Graduate School
Southern Illinois University

Morgan R. Muell

morganrmuell@gmail.com

Iowa State University
Bachelor of Science, Biology, May 2018

Special Honors and Awards:

Students United in Preserving, Exploring, and Research Biodiversity Fellowship 2019–2020
Zoology Summer Scholarship – June 2019

Thesis Paper Title:

Phylogenomic analysis of evolutionary relationships in *Ranitomeya* poison frogs (Amphibia: Dendrobatidae) using ultraconserved elements

Major Professor: Dr. Jason L. Brown

Publications:

Muell, M. R., A. L. Carter, and F. J. Janzen. In press. Modeling onset of hourly nesting activity in a freshwater turtle using abiotic variables and physiological capacity. Journal of Herpetology.

Muell, M. R., W. X. Guillory, A. Kellerman, A. O. Rubio, A. Scott-Elliston, O. J. Morales, K. Eckhoff, D. Barfknecht, J. Hartstock, J. J. Weber, and J. L. Brown. 2020. Gaming natural selection: using board games as simulations to teach evolution. Evolution 74:681–685.

Guillory, W. X., M. R. Muell, K. Summers, and J. L. Brown. 2019. Conservation and phylogenomic reconstruction of the Neotropical poison frogs (Dendrobatidae). Diversity 11:126.

Adams, C. I., L. H. Hoekstra, M. R. Muell, and F. J. Janzen. 2019. A brief review of non-avian reptile environmental DNA (eDNA), with a case study of painted turtle (*Chrysemys picta*) eDNA under field conditions. *Diversity* 11:50.

Muell, M. R. 2016. Geographic distribution: *Lampropeltis triangulum triangulum* (Eastern Milksnake). Herpetological Review 47:630.